A SURVEY OF SEPARATION PREDICTION METHODS APPLIED TO POTENTIAL FLOW SOLUTIONS FOR AN AIRFOIL

By

TAKAMASA KAI

Bachelor of Science

Keio University

Tokyo, Japan

1989

Submitted to the Faculty of the
Graduate College of the
Oklahoma State University
in partial fulfillment of
the requirements for
the Degree of
MASTER OF SCIENCE
JULY, 1995

A SURVEY OF SEPARATION PREDICTION METHODS APPLIED TO POTENTIAL FLOW SOLUTIONS FOR AN AIRFOIL

Thesis Approved:

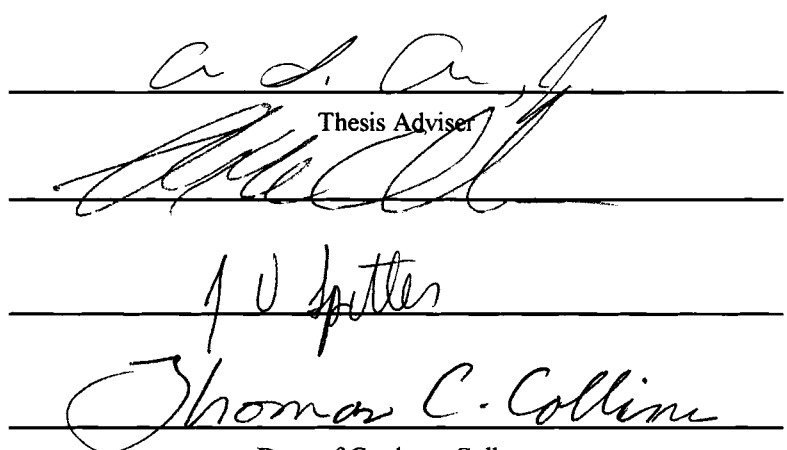

Thesis Adviser

Dean of Graduate College

PREFACE

This study was conducted to provide a new possible approach to the designing process of an airfoil. Four different computational separation prediction methods were used to investigate the separation characteristics of an airfoil. A panel method code was used to calculate the pressure distribution on each airfoil. By using a panel method as a tool to obtain the pressure distribution, which is to be used as input data for a prediction method code, the entire process of analysis of separation characteristics would be totally computational. And then, each airfoil can be analyzed in a short period of time so that it becomes possible to investigate a large number of airfoils in the process of designing an airfoil. Due to the invalidity of the pressure distribution calculated by Panel method where the angle of attack is large, however, the calculated results must be carefully taken into consideration with limitations in terms of Reynolds number, the angle of attack and an airfoil geometry.

I wish to express my sincere appreciation to my major adviser, Dr. Andrew Arena, for his intelligent supervision, constructive guidance, inspiration and friendship. My sincere appreciation extends to my other committee members, Dr. Frank Chambers and Dr. Jeffrey Spitler. I especially wish to thank Dr. Chambers for pointing out many mistakes regarding my English. I also thank my parents and Miss Chiyomi Seki for their support and encouragement.

TABLE OF CONTENTS

Chapter	Page
I. INTRODUCTION	1
1.1 Problem Statement	1
1.2 Background Literature Review	3
1.3 Summary	10
1.4 Objectives of the Present Investigation	11
II. BOUNDARY LAYER	13
2.1 Boundary Layer Equations	13
2.1.1 Boundary Layer	13
2.1.2 Laminar Boundary Layer	14
2.1.3 Turbulent Boundary Layer	16
2.2 Boundary Layer Transition	17
2.2.1 Boundary Layer Transition	17
2.2.2 Laminar Separation Bubble	18
2.2.3 Separation Bubble Warning	21
2.2.4 Boundary Layer Separation	21
III. COMPUTATIONAL METHODOLOGY	24
3.1 Boundary Layer Transition Criteria	24
3.1.1 Michel Criteria	24
3.1.2 Velocity Maximum Point	25
3.2 Separation Prediction Methods	26
3.2.1 Stratford's Method	27
3.2.2 Goldschmied's Method	30
3.2.3 Thwaites's Method	34
3.2.4 Head's Method	37
3.3 Effect of Boundary Layer Separation on Aerodynamic Characteristics	41
3.4 Computer Code	42
3.4.1 Stratford's method code	42
3.4.2 Goldschmied's code	43
3.4.3 Integral method code	45

Chapter Page

IV. RESULTS 47

4.1 The sharp pressure spike near the leading edge 47
4.2 Code validation where the angle of attack is small 50
4.2.1 Stratford's method 50
4.2.2 Goldschmied's method 51
4.2.3 Integral method (Thwaites-Head's combined method) 52
4.3 The region of high angle of attack 52
4.4 Corrected Cl, Cm by Integral method 57
4.5 Sensitivity survey for the use of Integral method 62
4.6 Transition criteria 64
4.7 Validity of the maximum velocity criterion with potential flow solutions 67
4.8 The code validity for low Reynolds number 72

V. CONCLUSIONS AND RECOMMENDATIONS 75

5.1 Conclusions 75
5.2 Recommendations 76

REFERENCES 78

APPENDIXES 80

LIST OF FIGURES

Figure page

2.1 Displacement effect of separation bubbles 20

2.2 Velocity profile within the boundary layer for favorable and adverse pressure gradients 23

3.1 Actual and 'equivalent' distribution of $\frac{q_e}{q_m} = \left(\frac{u_e}{u_m}\right)^2$, forming the basis for the laminar separation calculation 27

3.2 Concept of entrainment 38

4.1 The chord-wise pressure distributions obtained by potential flow calculation and observed in experimental data (NACA4412, α=8°, Re=3,000,000) 48

4.2 The chord-wise pressure distributions obtained by potential flow calculation and observed in experimental data (NACA4412, α=16°, Re=3,000,000) 49

4.3 The chord-wise pressure distributions obtained by potential flow calculation and observed in experimental data (NACA4412, α=24°, Re=3,000,000) 49

4.4 Calculated separation point with small angle of attack 0°-7° 51

4.5 Calculated characteristics of separation with high angle of attack on NACA4412 53

4.6 Calculated characteristics of separation with high angle of attack on NACA0012 53

4.7 Corrected Cl, Cm on NACA747A315 (Re=6,000,000) 58

4.8 Corrected Cl, Cm on NACA63$_2$-415 (Re=6,000,000) 58

Figure page

4.9 Corrected Cl, Cm on NACA63A210 (Re=6,000,000) 59

4.10 Corrected Cl, Cm on NACA0012 (Re=1,800,000) 59

4.11 Corrected Cl, Cm on NACA1408 (Re=9,000,000) 60

4.12 Corrected Cl, Cm on NACA4412 (Re=3,000,000) 60

4.13 Corrected Cl, Cm on NACA64-108 (Re=6,000,000) 61

4.14 Corrected Cl, Cm on NACA2412 (Re=5,700,000) 61

4.15 The predicted separation points by integral method with the varied starting value of H for the turbulent boundary layer (NACA0012, Re=1,800,000) 63

4.16 The predicted separation points by integral method with two different transition criteria. Calculations are based on the pressure distribution from experimental data (NACA4412, Re=3,000,000) 65

4.17 The predicted separation points by integral method with two different transition criteria. Calculations are based on the pressure distribution from potential flow theory (NACA4412, Re=3,000,000) 66

4.18 The predicted separation points by integral method with two different transition criteria. Calculations are based on the pressure distribution from potential flow theory (NACA0012, Re=1,800,000) 66

4.19 The change of the location of separation point with the location of transition. "**M**" denotes the point of the maximum velocity (NACA0012, Re=1,800,000) 69

4.20 The change of the location of separation point with the location of transition. "**M**" denotes the point of the maximum velocity (NACA4412, Re=3,000,000) 70

4.21 The change of the location of separation point with the location of transition. "**M**" denotes the point of the maximum velocity (NACA63_2-415, Re=6,000,000) 71

Figure page

4.22 Location of separation points on a circular cylinder as a function of Reynolds number 74

A.1 Code validation with NACA4412, Re=3,000,000 99

A.2 Code validation with NACA65,2-421, Re=6,000,000 100

A.3 Code validation with NACA66,2-420, Re=6,500,000 100

NOMENCLATURE

c	chord length
C_f	skin friction coefficient
C_{fm}	skin friction coefficient at the point of the minimum pressure
c_l	sectional lift coefficient
Δc_l	change of c_l due to separation
c_m	sectional moment coefficient
Δc_m	change of c_m due to separation
Cp	pressure coefficient
$\overline{C_p}$	pressure coefficient in terms of the minimum pressure
C_{psep}	pressure coefficient at separation point
E	entrainment velocity
H	shape factor = δ*/θ
H1	$= \frac{\delta - \delta^*}{\theta}$
h_c	constant total head
h_m	total head at the point of the minimum pressure

L body length

l $= \frac{\rho V_e \theta}{2\mu} c_f$

p pressure

$\overline{p}$ time-averaged p

Q volume rate of flow within the boundary layer

Re Reynolds number in terms of U and c

Re_θ Reynolds number in terms of θ

Re_x Reynolds number in terms of x

$\overline{\mathrm{Re}}$ Reynolds number in terms of the maximum velocity and $\overline{x}$

S Stratford coefficient

S_{sep} distance of separation point from the trailing edge

U freestream velocity

U(x) potential flow velocity distribution

$U_B(x)$ velocity distribution with the presence of separation bubble

U_S velocity at separation point

$\dot{U}_0$ velocity gradient at the leading edge stagnation point

ΔU_B velocity difference between the separation point and the reattachment point

u velocity component of x direction, or the tangential velocity component to an airfoil surface

$\overline{u}$ time-averaged u

u' fluctuating quantity of u

u^* frictional velocity of u

u_m^* frictional velocity of u at the minimum pressure point

u_t u at transition point

v velocity component of y direction, or the normal velocity component to an airfoil surface

$\bar{v}$ time-averaged v

v' fluctuating quantity of v

V_e the outer edge velocity of the boundary layer

x distance from the forward stagnation point

x_t distance of transition point from the forward stagnation point

x_m distance of the point of the minimum pressure from the forward stagnation point

x_s distance of separation point from the forward stagnation point

$\overline{x_m}$ distance from the forward stagnation point under the 'fictitious' constant pressure distribution necessary to develop the same θ seen at x_m under the 'actual' pressure distribution

$\bar{x}$ $= x - x_m + \overline{x_m}$ *where* $x \geq x_m$

y distance from an airfoil surface

y_c distance of assumed constant total head line from an airfoil surface

u_c mean u within the boundary layer at $y=y_c$

α angle of attack

$\Delta\alpha$ change of α due to separation

δ boundary layer thickness

δ^* displacement thickness

λ $= \frac{\rho\theta^2}{\mu}\frac{dV_e}{dx}$

μ coefficient of viscosity

θ momentum thickness

ρ density of mass

τ_w shear friction at wall

CHAPTER I

INTRODUCTION

1.1 Problem Statement

In designing airfoils, it is necessary to know whether the boundary layer, either laminar or turbulent, will separate from the surface of the airfoil being developed. Characteristics of an airfoil largely depend on its degree of separation occurring and significant efforts have been made by many researchers to prevent the boundary layer from separation or, if it separates, improve its separation characteristics. To design efficient airfoils or hydrofoils, it is important to avoid flow separation to keep drag levels low, and it is also crucial for one developing an airfoil with high-lifting capability to examine the separation characteristics.

The point of separation can be studied experimentally with the wind tunnel by plotting the pressure distribution along the surface over the airfoil. The presence of separation causes the pressure distribution to be approximately constant after the point of separation. Therefore, by observing the pressure distribution carefully in varied angle of attack, the Reynolds number etc, one is able to investigate the separation characteristics of the airfoil being studied. Many prediction methods have been introduced. Some of

them require detailed boundary layer solution, while others use a single or only a few parameters. The boundary layer information required by these methods can appropriately be obtained through the wind-tunnel type experiment, for the information obtained by the experiments is, indeed, what exactly is happening in the "real" flow.

Searching for the point of separation by a prediction method with the boundary-layer data obtained experimentally may, however, be considered unreasonable. Suppose one is investigating the separation point with some prediction calculation , say a simple method such as Stratford's method, acquiring the experimental pressure distribution at the first place, one already knows or can reasonably guess the location of separation by locating the point where the flattened pressure distribution starts. Therefore, using the single parameter method like Stratford's method to predict the separation point may seem absurd since one might already be able to tell whether or where flow separates before using the prediction method.

The boundary-layer information can also be derived as potential flow solution by inviscid theory, which should be done faster and easier because it doesn't require any experiment facility but computer. It is well known that potential flow solution is not always reasonable enough to describe "real" flow field, which does have viscosity. Especially as the angle of attack gets larger, the magnitude of the sharp pressure spike at near the leading edge, which is known as the characteristics of inviscid solution, becomes more unrealistically noticeable compared to experimental data. Consequently where the angle of attack is large enough, there should always be a difference between the boundary-layer data obtained by a experiment and those calculated with potential flow

theory. Despite this fact, it is also true that where the angle of attack is relatively small, potential flow solution may have a good agreement with experimental data so that there should be a range of the angle of attack where easily-obtained potential solutions can be used with separation methods in order to design an efficient airfoil. Moreover, to design an airfoil for certain purpose by 'trial-and-error' type process, the possible usage of potential flow solution can be time-saving as a number of experiments are not necessary to be conducted for each slight change of shape of an airfoil. Thus Investigating the region where potential flow solution can be close enough to experimental data and to what extent the predict methods can predict the point of separation with reasonable accuracy helps researchers developing an airfoil of high-lifting capability.

1.2 Background Literature Review

In the literature survey done for the current study, several separation prediction methods have been reviewed. In the process of designing an airfoil, one may not be interested in the boundary layer solutions as in detailed as would be obtained by experiment, and also one may not want to spend the considerable time required to obtain such detailed solutions. This process can be avoided by using an appropriate computational method which is the most suitable for one's purpose.

There would appear to be three things which might determine the choice of method. First, the question arises as to how much information is required. For

example, it is desired merely to calculate the position at which the boundary layer separates, or $\delta*$, or θ at various points along the surface of the airfoil? or , on the other hand, is it required to obtain an accurate estimate of the detailed manner in which the velocity profile within the boundary layer develops? Second, the question of accuracy arises. Is a rough estimate, say within 5 percent, adequate or is it essential to calculate some property or other within 5 percent at most ? Thirdly, when those methods have been rejected which do not match up to the requirements on these two counts, the choice between remainders can be determined by questions of speed and simplicity.

With high-speed computers, the governing boundary layer equations for the laminar flow can be solved exactly, and consequently, the laminar separation point can be determined almost exactly. In addition, there are several computational methods which still can be used to predict separation points quite satisfactorily.

<< The Prediction Methods Studied >>

For Laminar Boundary Layers

Detailed Boundary Layer Solutions to be obtained

- Pohlhausen's Method .....Integral-Type
- Thwaites's Method .....Integral-Type

No Detailed Boundary Layer Solutions to be obtained

- Stratford's Method .....Simple-Type

For Turbulent Boundary Layers

Detailed Boundary Layer Solutions to be obtained

- Head's Method .....Integral-Type
- Cebeci-Smith's Method ....Differential-Type

No Detailed Boundary Layer Solutions to be obtained

- Stratford's Method .....Simple-Type
- Goldschmied's Method .....Simple-Type

Pohlhausen's [14], Thwaites's [1], and Stratford's [2] methods are examples of three such methods. Stratford's method does not even require the laminar boundary layer solutions. Using these method, the skin friction distribution is to be sought and any of these method is satisfactory, with the qualification that for flow which starts from a stagnation point, which is the case of an airfoil rather than a sharp leading edge [14].

Pohlhausen's method was historically the first general method to be developed. In this method, the boundary layer equations are not satisfied everywhere ,but are satisfied at the wall and at the outer edge of the boundary layer. The velocity profile within the boundary layer is assumed to take a polynomial form, and then the skin-friction τ_w, the displacement thickness δ^*, and the momentum thickness θ are to be calculated. With a polynomial-form velocity profile, the boundary condition both at the wall and the outer edge of the boundary layer are to be satisfied. Assuming the outer edge velocity distribution is known beforehand, the boundary layer thickness is to be determined. Pohlhausen's method yields accurate results in a favorable pressure gradient region, but becomes less accurate as separation is approached, so that the predicted distances to separation are typically 30% too high [14].

Thwaites pointed out that if one wishes to calculate only the boundary thickness and the skin-friction distribution, it is not necessary to introduce explicit assumptions concerning detailed velocity profile within the boundary layer as Pohlhausen's method does. If suitable correlations are defined between the overall boundary layer characteristics, one can easily obtain λ, eq.(3.11), as a function of x, after which θ, δ, H

and c_f follow. This is the concept on which Thwaites's method is built. The method will be explained in detail later.

The method developed by Stratford is based on the idea of dividing the boundary layer into the outer and inner regions, for each of which a solution is obtained which joins smoothly onto the other [14]. Stratford's method is only used downstream of the point of the minimum pressure. If any more detailed information is required, Stratford's method, a simple 'one-parameter' method, must be rejected, while the other two methods are able to give $\delta*$, θ and H. These method are almost equally accurate [14]. Regarding simplicity, Stratford's method is far simpler than the others.

Unlike the case of the laminar boundary layer, the prediction of the separation point in the turbulent boundary layer is far more difficult task. As a result of the presence of the time mean of the fluctuating quantities appearing in the government equations, an exact solution of the turbulent boundary layer is impossible to obtain.

The currently-known separation prediction methods for the turbulent boundary layer can be divided into two groups. In one group are the methods that require the detailed boundary layer solutions. These methods are either of differential type or of integral type. Cebeci-Smith's method [18] and Head's method [12] are well known as a differential-type method and an integral-type method respectively. The zero wall stress is used to predict the separation point in differential methods, while the shape factor is usually used in integral methods.

Cebeci-Smith's method is a finite-difference method for solving laminar and turbulent boundary layer equations for incompressible and compressible flows about two-dimensional and axisymmetric bodies [18].

Head's method is an integral method which is based on the concept of an entrainment velocity. Head assumed that the dimensionless entrainment velocity E/V_e depends only on H, and that H_1, in return, is a function of H. Then, the momentum equation, entrainment relation, shape factor relation, and Ludwieg-Tillman skin-friction law are used for four unknown θ, H, H_1 and c_f.

In the other group are methods that do not require detailed boundary layer calculation. With these method, the point of separation is predicted by simple formula, or by simple differential equations. Stratford's [2] and Goldschmied's [5] methods are the methods of this type.

As mentioned before for the case of the laminar boundary layer, if any detailed boundary layer information is required, neither Stratford's method nor Goldschmied's method is the right choice. Either differential or integral type method must be used for such a case. As for simplicity, Goldschmied's method is the best of all, followed by Stratford's method. Goldschmied's method, however, is said to be inconclusive especially when applied to the airfoil-type pressure distribution [19]. Additionally, it is known that Stratford's tends to predict 'early' separation but results are still reasonable. Compared to experimental data, Cebeci-Smith's method is quite accurate, though these methods are far more complicated and not easy to code [18].

For the current study, three methods are used, two 'simple' methods and one 'detailed' method. These simple ones are Stratford's method and Goldschmied's method. Simple methods, from which detailed boundary layer parameter cannot be obtained is considered suitable for this study. In this survey, the location of separation point is mainly focused on and any detailed boundary layer solutions are not quite necessary to know. In addition to it, of course, its simplicity can be found favorable from airfoil designer's point of view. As for simplicity, Goldschmied's method was first chosen because it is the simplest one of all I have looked into. Goldschmied's method, however, is said to be inconclusive when applied to airfoil-type pressure distribution, as a result of the very questionable assumption concerning the constant total head at the edge of the viscous layer [19]. At the edge of the viscous layer, the total head actually is not constant but either increasing or decreasing, depending on a place one is looking at [5]. Furthermore, it is known that this assumption can be doubtful when the adverse pressure gradient is large [5], which is the case of potential flow solution for an airfoil.

In addition to Goldschmied's method, the well-known method of Stratford's was additionally chosen to be used. Unlike Goldschmied's method, Stratford's method may be applied to any given pressure distribution [2] and is known to be accurate, while it tends to predict 'early' separation [19].

Two integral-type methods, Thwaites's method and Head's method, were selected as well. Actually, two method were put in one program, where Thwaites's method was used for laminar boundary layers and Head's method for turbulent boundary layers.

As a differential-type method, Cebeci-Smith's method was looked into as well, but not used for the current study. Cebeci-Smith's method is the method which is able to handle both laminar and turbulent for incompressible and even compressible. This differential method is so flexible that the method is far more complicated than any other ones studied. On the other hand, however, it is studied that the accuracy of Cebeci-Smith's method is usually no more than that of Head's method, an integral-type method [19]. Head's method already being chosen, therefore, it was concluded that it is not worth using the 'complicated' method of Cebeci-Smith's, which is no better than an integral-type method in most cases.

As for the use of potential flow solutions for boundary layer analysis, In [10], coupling between potential flow and boundary layer solvers is suggested. This idea requires the boundary of surface for the potential flow boundary conditions to be raised by δ^*. To do this, the following procedure is necessary.

Firstly, the potential flow field over the body is solved so that the surface pressure distribution, or velocity, distribution is obtained. Secondly, based on the results obtained in the first step, δ^* will be calculated. Then, thirdly, the surface boundary is modified by shifting the surface by δ^*. After that, the next iteration is to be done with modified geometry, and the iteration should be repeated until solutions converge.

In the case of an airfoil, however, it has been studied that in the current survey that the magnitude of δ^* has been found as small as less than 8% of the maximum thickness ratio of most of airfoils studied here, moreover, where there is a favorable pressure gradient, δ^* is even as thin as less than 0.8%.

With this fact, it can hardly be critical to take into account the change of the body geometry due to δ^*. Therefore, solving the coupled potential flow and boundary layer equations were neglected and the boundary of body is left as it is, which possibly saves significant computation time. Since the sharp pressure drop near the leading edge in potential flow solutions for an airfoil was expected, in the current study, an integral-type method takes an important role. to overcome the pressure spike expected to be seen in potential flow solutions for an airfoil. Even though there should be a sharp pressure drop, which makes pressure distribution based on potential flow theory differ from experimental data, the effect caused by this sharp spike is confined within narrow range in terms of chord-wise direction. Therefore, using an integral-type methods, the effect of a sharp pressure drop can be kept as small as possible in the process of integrating the momentum equation in x-direction. So, as seen later, choosing an integral method will be found successful.

1.3 Summary

In the process of designing an efficient airfoil, it is a crucial part to investigate aerodynamic characteristics of the airfoil being developed. Among many elements affecting an airfoil's efficiency, the occurrence of separation should be focused on as it is greatly responsible for the dynamic loading and then resulting motion. In this sense, the

wind tunnel experiment is needed to be done. The data collected from the wind tunnel is, of course, 'real' and helpful to see what is happening in the flow field around the airfoil and therefore, it exactly tells what is going on within the boundary layer on its surface. So that conducting the wind tunnel experiment, one can sufficiently examine the effectiveness of the airfoil and see how the airfoil may be more improved. Other than the wind tunnel, one may consider some computational methods as tools to examine an airfoil. Unlike the wind tunnel case, calculation required for estimation needs neither the large-scale experimental facility nor large amount of time to prepare for each experiment, and it can be done even with a personal computer at home. Especially if the airfoil is being developed with the 'Trial-and Error' type, or 'The survival of the fittest' - like, procedure, setting up the wind tunnel for each wing of slight difference may be time-consuming. It is well known, however, that as the angle of attack becomes larger, the calculated aerodynamic loading will not be able to describe the 'actual' aerodynamic loading so that over a certain value of the angle of attack, the data obtained from potential flow theory should be given up unless the computational method, which is capable of overcoming the difference and still reasonably estimate the airfoil, or at least showing the tendency of the aerodynamic characteristics of it being interested does exist.

1.4 Objectives and the Present Investigation

It is some of interest to know to what extent potential flow theory models may be applied to an airfoil in order to simplify the process to analyze separation characteristics. In this connection, it is also important to examine what kind of separation prediction method should be used to predict the location of separation with reasonable accuracy, when applied to potential flow solution. Expecting the difference, does sharp pressure drop near the leading edge seem in potential flow data but in experimental data make the usage of the pressure distribution based on inviscid theory totally invalid? Does any separation prediction method overcome the pressure-spike mentioned above and still show the results adequately closer to those obtained experimentally. Specifically, in order to address these questions the following investigation have been performed.

1) Transition criteria are studied and their validations are examined.

2) Applicability of two single parameter-type methods and an integral-type method to potential flow solutions is studied, and fundamental differences between them are discussed.

Accordingly, the objectives of the current study are to ascertain the region, in terms of the angle of attack, where potential flow data can be used for analysis of the separation characteristics and to investigate the validity of prediction methods against the high pressure gradient caused by leading edge pressure drop.

CHAPTER II

THE BOUNDARY LAYER

2.1 The Boundary Layer

2.1.1 The Boundary Layer

In the flow field with the high Reynolds number, viscosity can be ignored and then flow can be considered as ideal flow. With an object immersed in such a flow, however, this simplification cannot be applied to the region close to the object and wake shed from the object. If there is an object immersed in such a flow, due to non-slip condition, the velocity gradient, $\partial u/\partial y$, becomes large in the region very close to its surface, and the effect of viscosity must be taken into account. Therefore, when the Reynolds number is large enough, it is convenient to divide the flow field being investigated into two portions, the region close to the object and the region distant from it. The former is called the boundary layer.

There are three important parameters to know, which characterize the boundary layer,

$$\delta^*(x) \equiv \int_0^\infty \left[1 - \frac{u(x,y)}{V_e(x)}\right] dy \tag{2.1}$$

is called the 'displacement thickness', δ* of the boundary layer. This is the distance the external flow stream lines are displaced by the boundary layer. Another useful parameter is the 'momentum thickness',θ ,

$$\theta \equiv \int_0^\infty \frac{u(x,y)}{V_e}\left[1 - \frac{u(x,y)}{V_e}\right] dy \tag{2.2}$$

The last parameter is the 'shape factor', H, defined as below,

$$H \equiv \frac{\delta^*}{\theta} \tag{2.3}$$

2.1.2 The Laminar Boundary Layer Equation

It is assumed that the radius of the curve of the object being studied is large enough, which is the case of an airfoil, then with x measured normal to the surface and y measured parallel to it, as is the case of Cartesian coordinate, the Navier-Stokes equations and the continuity equation describing flow field within the boundary layer are:

$$\frac{\partial u}{\partial t} + u\frac{\partial u}{\partial x} + v\frac{\partial u}{\partial y} = -\frac{1}{\rho}\frac{d\,p}{d\,x} + \nu\left(\frac{\partial^2 u}{\partial x^2} + \frac{\partial^2 u}{\partial y^2}\right) \tag{2.4}$$

$$\frac{\partial v}{\partial t} + u\frac{\partial v}{\partial x} + v\frac{\partial v}{\partial y} = -\frac{1}{\rho}\frac{d\,p}{d\,y} + \nu\left(\frac{\partial^2 v}{\partial x^2} + \frac{\partial^2 v}{\partial y^2}\right) \tag{2.5}$$

$$\frac{\partial u}{\partial x}+\frac{\partial v}{\partial y}=0 \tag{2.6}$$

Considering the nature of the boundary layer, some of terms in these equations may be omitted as the magnitudes of some terms are very small, compared to those of the other terms. Integrating the continuity equation, eq.(2.6), with no-slip condition at the wall as the boundary condition gives:

$$v=-\int_0^y \frac{\partial u}{\partial x}dy \tag{2.7}$$

In the case of an airfoil, the chord length, L, the freestream velocity, U, and the boundary layer thickness, δ, are used to examine the magnitude of each term.

$$\frac{\partial u}{\partial x}\approx\frac{U}{L} \; and \; y\approx\delta$$

Therefore from eq.(2.7),

$$v\approx U\frac{\delta}{L}$$

Then, since L >> δ, the magnitude v should be smaller that that of u. Therefore, u-related terms in eq.(2.5) can be omitted and

$$\frac{\partial p}{\partial y}\approx 0 \tag{2.8}$$

So that p is independent of y and the pressure distribution along the outer edge of the boundary layer calculated by potential flow theory can then be used as the pressure distribution on the surface of the object. The other terms' magnitudes may be examined as well, finally the governing equations for flow within the laminar boundary layer are:

$$\frac{\partial u}{\partial t}+u\frac{\partial u}{\partial x}+v\frac{\partial u}{\partial y}=-\frac{1}{\rho}\frac{dp}{dx}+\nu\left(\frac{\partial^2 u}{\partial x^2}+\frac{\partial^2 u}{\partial y^2}\right)$$

$$0=\frac{dp}{dy} \qquad (2.9)$$

$$\frac{\partial u}{\partial x}+\frac{\partial v}{\partial y}=0$$

In the case of an airfoil with Re > 10^5, the value of δ^* is very small, in other words, the boundary layer is so thin that the existence of the boundary layer thickness can be ignored. Therefore, potential flow solutions along the outer edge of the boundary layer can be shifted to an airfoil surface and used as solutions directly on the surface of the airfoil.

2.1.3 The Turbulent Boundary Layer Equation

The local Reynolds number based on the distance from the forward stagnation point over the surface of the airfoil becoming larger and the point of the instability reached, any small disturbance within the laminar boundary layer can wildly amplified. The flow is unstable and indicates a time-dependence. The boundary layer entering these states is called 'the turbulent boundary layer'. It is still governed by Navier-Stokes equations and the continuity equation in respect of time-averaged terms.

$$\rho\left(\bar{u}\frac{\partial\bar{u}}{\partial x}+\bar{v}\frac{\partial\bar{u}}{\partial y}\right)=-\frac{\partial\bar{p}}{\partial x}+\frac{\partial}{\partial x}\left(\mu\frac{\partial\bar{u}}{\partial x}-\rho\overline{u'^2}\right)+\frac{\partial}{\partial y}\left(\mu\frac{\partial\bar{u}}{\partial y}-\rho\overline{u'v'}\right) \qquad (2.10)$$

$$\rho\left(\bar{u}\frac{\partial\bar{v}}{\partial x}+\bar{v}\frac{\partial\bar{v}}{\partial y}\right)=-\frac{\partial\bar{p}}{\partial y}+\frac{\partial}{\partial x}\left(\mu\frac{\partial\bar{v}}{\partial x}-\rho\overline{u'v'}\right)+\frac{\partial}{\partial y}\left(\mu\frac{\partial\bar{v}}{\partial y}-\rho\overline{v'^2}\right) \tag{2.11}$$

$$\frac{\partial\bar{u}}{\partial x}+\frac{\partial\bar{v}}{\partial y}=0 \tag{2.12}$$

These equations contain derivatives of terms of the form

$$-\rho\,\overline{v_i' v_j'}$$

which are called 'Reynolds stress' or 'turbulent shear stress'.

2.2 Boundary Layer Separation

2.2.1 Boundary Layer Transition

In the case of the boundary layer starting out as laminar flow, flow near the surface goes over the surface of the airfoil. Sooner or later, the point of instability is reached then the boundary layer becomes unstable and turns into turbulent layer. Transfer occurs at a certain value of the Reynolds number based on the distance from the point where the boundary layer started, or the leading edge stagnation point for an airfoil case, depending on many other factors. Two factors are especially important among them, the pressure gradient and the surface roughness. In other words, transition can be hastened by both surface roughness and a positive pressure gradient, or adverse pressure gradient.

2.2.2 Laminar Separation Bubble

It is well known that the laminar boundary layer needs much less adverse pressure gradient than the turbulent case to separate from the surface it flows over. Unlike the laminar boundary layer, in the turbulent boundary layer, there is energy exchange between the inner region and the outer region within the boundary layer, and high kinetic energy in the outer region can be transferred to the inner region and help flow going against adverse pressure gradient without separation. Without this energy exchange, laminar separation occurs much earlier and causes a lager wake than the turbulent one. Once flow separates, skin friction becomes smaller while profile drag gets significantly larger. Concerning the magnitudes of these two drag, the latter is dominant, and therefore, the laminar boundary layer separation results in the high drag after all. One can directly prevent this high drag caused by laminar separation by having the point of transition before the point where laminar separation is expected to occur. In this way, the laminar boundary layer reattaches as the turbulent boundary layer, which continue to follow the surface until it finally separate somewhere downstream. As seen below in Michel criterion formula eq.(3.2),

$$\mathrm{Re}_\theta > 1.174\left(1+\frac{22400}{\mathrm{Re}_x}\right)\mathrm{Re}_x^{0.46} \qquad (3.2)$$

The point of transition largely depends on the local Re_θ ,and transition can be promoted by increasing $\theta(x)$, which is all can be deduced by observing the formula of Michel

criterion above. Increasing $\theta(x)$ can be done by changing the velocity profile within the boundary layer and the pressure gradient has strong influence on the velocity profile. There, however, is the well-known fact that separation may also occur in transition region, which the code developed for the current study cannot take into account. This is particularly likely, mainly if a strong adverse pressure gradient is present there, and this is exactly the case of an airfoil, especially with potential flow solutions. Moreover, in the case of separation during transition, a short wake exists where the pressure is constant, a free shear layer is present between the wake and the potential, or outer, flow. This shear layer is much more unstable than the boundary layer along the wall because the wall has a damping effect so that 'the second' transition into the turbulent layer occurs in the free shear layer shortly after separation during 'the first' transition. Turbulence spreads and the thickness of the turbulent shear layer increases. It may reach the surface again, which means turbulent reattachment occurs. An attached turbulent boundary layer is the continuation. This phenomenon is called a laminar separation bubble. The separation bubble is one of the most significant phenomena affecting the characteristics of airfoils.

If there is no reattachment, hence no separation bubble, occurring, then the laminar boundary layer simply separates from the surface. Thus, the large wake region will be formed, which turns into the vortex motion causing a large profile drag. Consequently, very poor airfoil characteristics will be observed.

On the other hand, if reattachment, hence the separation bubble, occurs, the difference between early and late reattachments is also very important. The thickness of

the turbulent shear layer increases at much higher rate than that of the turbulent boundary layer. Therefore, late reattachment causes a much thicker initial turbulent boundary layer, early turbulent separation and much more drag than early reattachment.

Another feature of the separation bubble is a displacement effect on the velocity distribution, and this is sketched in Figure 2.1. The solid line U(x) denotes the potential flow velocity distribution while the broken line shows the velocity distribution $U_B(x)$,if the separation bubble is present. It is known that after the separation, there will be a constant pressure region. This region continues until the shear layer transition T. Then, $U_B(x)$ drops more steeply then U(x) and after a reduction ΔU_B of $U_B(x)$, the original distribution U(x) is intersected at the reattachment R. The value of ΔU_B is to be used for the bubble warning, which is to be explained in the following section.

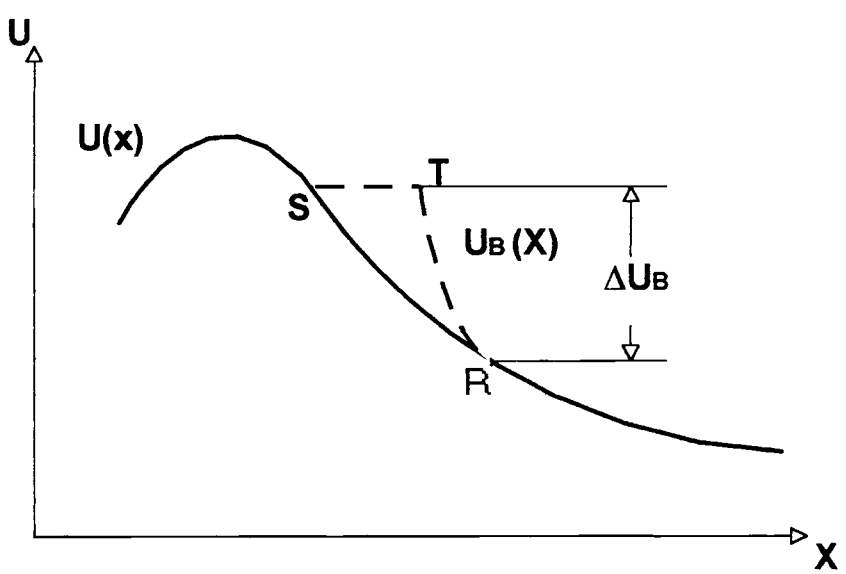

Figure 2.1. Displacement effect of separation bubbles [15]

2.2.3 The Bubble Warning [15]

There is often a large difference between computed drag and experiment drag, and this is frequently due to a separation bubble. The best way to account for the bubbles in the boundary layer could be, of course, an empirically determined drag penalty. This has not been attempted, because there are at the present time insufficient systematic experimental results. Instead, an empirical criterion was developed which gives a warning if additional drag from the bubble region must be expected. Such a criterion is very helpful for airfoil design purposes. Based upon many experiments the warning is to be given if [15]

$$1-\frac{\Delta U_B}{U_S}=0.958 \tag{2.13}$$

The criterion has been successfully applied in many cases, and it is known as the normal criterion for computation of boundary layers.

2.2.4 Boundary Layer Separation

In the preceding section, the equations governing the flow within the boundary layer have been introduced as follows,

$$\frac{\partial u}{\partial t} + u\frac{\partial u}{\partial x} = -\frac{1}{\rho}\frac{dp}{dx} + \nu\left(\frac{\partial^2 u}{\partial x^2} + \frac{\partial^2 u}{\partial y^2}\right)$$

$$0 = \frac{dp}{dy} \qquad (2.9)$$

$$\frac{\partial u}{\partial x} + \frac{\partial v}{\partial y} = 0$$

Considering the inner region within the boundary layer, flow there is strongly affected by the existence of the wall. In this region, both u and v are very small and flow is mainly governed by the equation below.

$$u \approx 0 \quad and \quad v \approx 0$$

therefore,

$$\frac{\partial^2 u}{\partial y^2} = \frac{1}{\mu}\frac{dp}{dx} \qquad (2.14)$$

Therefore, when dp/dx <0, or favorable pressure gradient, $\partial^2 u/\partial y^2 < 0$ when dp/dx >0, or adverse pressure gradient, $\partial^2 u/\partial y^2$ becomes otherwise.

In general, the point of the minimum pressure is found somewhere on the surface on the surface of the object being studied. Before the point, dp/dx <0, and after the point, dp/dx >0. Downstream of the point of the minimum pressure, flow is decelerated. Being decelerated to certain extent, the boundary layer cannot continue going against adverse pressure gradient so that there will be the region where there is a adverse flow, fluid flowing toward the leading edge from the trailing edge. Once the value of $\partial u/\partial y$ reaches 0 or zero skin skin friction occurs, the boundary layer is no longer able to flow along the surface and then separates from it. For the laminar boundary layer separation, the point where $\partial u/\partial y$ reaches 0 is used as the separation criterion.

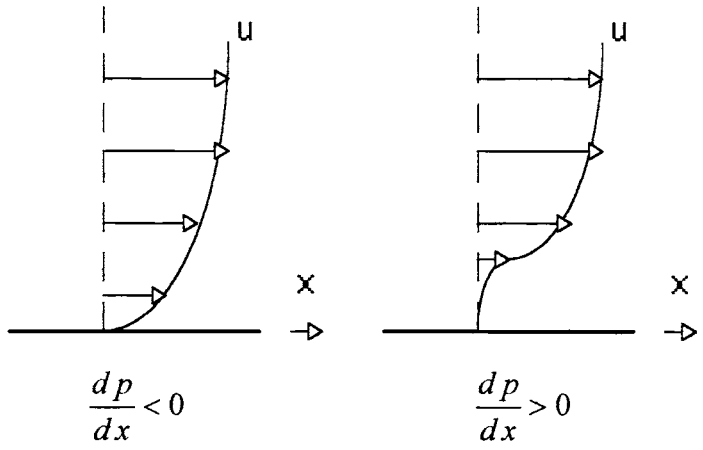

Figure 2.2. Velocity profile within the boundary layer for favorable and adverse pressure gradients

In the case of the turbulent boundary layer flow, flow in the boundary layer has large kinetic energy so that the boundary layer can be more resistant than the laminar boundary layer against adverse pressure gradient. Unlike the laminar boundary layer case, the shape factor H is generally considered as the separation criterion for the *turbulent boundary layer separation [12].*

CHAPTER III

COMPUTATIONAL METHODOLOGY

3.1 Boundary Layer Transition Criteria

3.1.1 Michel Criterion

For the case of flow past an airfoil, the boundary layer starts out as laminar and the initial value of the momentum thickness can be shown to be [12]:

$$\theta = \sqrt{\frac{0.075\mu}{\rho \dot{V}_0}} \qquad \text{at the leading edge stagnation point} \qquad (3.1)$$

And then, as it goes farther over the airfoil surface, the boundary layer becomes turbulent. Transition occurs at a particular value of the Reynolds number based on the distance x measured along the surface from the starting point of the boundary layer, which in an airfoil case is the leading edge stagnation point. For the boundary layer on a smooth flat plate, the critical value of the Reynolds number Rex is about 2,800,000, depending on the turbulence in the onset flow. In fact, the value of transition Reynolds number can be affected by a number of factors as mentioned before. For incompressible

flows without heat transfer, Michel suggested the criterion of the transition point for airfoil-type applications as [12]:

$$\mathrm{Re}_\theta > 1.174\left(1+\frac{22400}{\mathrm{Re}_X}\right)\mathrm{Re}_X{}^{0.46} \tag{3.2}$$

Since this formula doesn't include the effect of surface roughness, which is also very important, this is not reliable for every application. However, it is known that this criterion should be good for wing analysis [12].

3.1.2 The Velocity Maximum Point

In the case of the flow past an airfoil, the boundary layer starts out as laminar at the leading edge stagnation point. As flow goes farther along the surface of an airfoil, the boundary layer reaches the point of instability and then becomes unstable. After that any small disturbance initiates transition to turbulence. For an airfoil, the location of the point of instability should be considered in terms of the angle of attack, the Reynolds number and the pressure distribution. It seems that as the angle of attack increases, the sudden pressure drop near the leading edge becomes prominent and the point of the minimum pressure on the suction side moves forward, closer to the leading edge. This tendency is so obvious that at early stage that once the value of the Reynolds number reaches a certain value, then, almost regardless of the Reynolds number, the point of instability hardly moves right in front of the point of the minimum pressure. Therefore,

the point of transition to the turbulent boundary layer is convincingly assumed to exist at the minimum pressure point or the maximum velocity point.

Schlichting [8] mentioned that it is seen that in the cases of airfoils, as the angle of attack increases, the minimum of pressure on the suction side more and more prominent, and simultaneously the point of instability, therefore the transient point, closes up towards the point of the minimum pressure, or the point of the maximum velocity, for all Reynolds numbers because steep course of the curve near the minimum pressure point. The discussion in [8] also leads to the conclusion that the theory of the stability shows that the pressure gradient exerts an overwhelming influence on the stability of the laminar boundary layer: a decrease in pressure in the downstream direction has a stabilizing effect, whereas a increasing pressure leads to instability. Consequently the position of the point of the maximum velocity influences decisively the position of the point of the instability, and therefore the point of transition. It can be assumed, as a rough guiding rule that at medium Reynolds number ($10^6 - 10^7$), the point of transition coincides with the point of the maximum velocity. The Reynolds number $10^6 - 10^7$ mentioned above is exactly the range where airfoils were investigated in the current study. Thus, the use of the velocity maximum point transition criterion has been considered justified [8], [12].

3.2 Separation Prediction Methods

3.2.1 Stratford's Method

Stratford's method is a rapid simple method for the prediction of flow separation requiring only a single parameter, pressure. The method tends to predict 'early' separation [19]. The advantage of this method is its simplicity as well as relatively good accuracy. Unlike Integral-type methods, it doesn't require detailed boundary layer solutions and the locations of separation calculated by this method can be nearly as accurate as those predicted by Integral-type method. The method is easy to implement into the code.

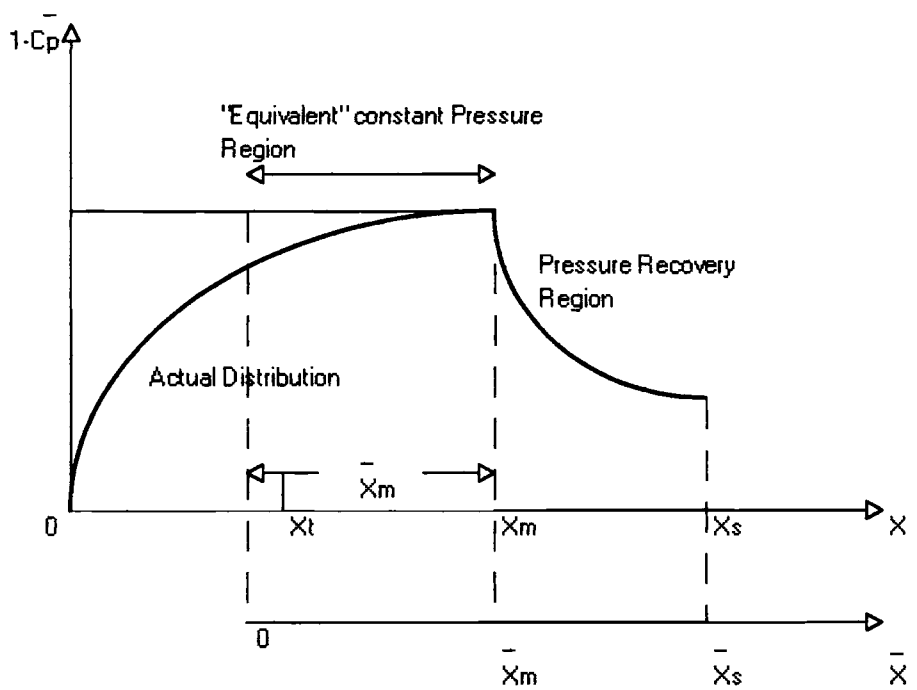

Figure 3.1. Actual and 'equivalent' distributions of $\frac{q_e}{q_m} = \left(\frac{u_e}{u_m}\right)^2$, forming the basis for the laminar separation calculation. [1]

Stratford's method is one of the simplest methods for locating the separation point for incompressible flow over a two-dimensional surface. The method only requires the pressure distribution over whatever surface it is applied to. Figure 3.1 shows essential features of the flow on which the analysis is based. x is measured from the stagnation point, $\overline{x_m}$ is the length of a constant pressure surface on which a boundary layer will develop a momentum thickness equal to that developed by the laminar, then turbulent boundary layer over the distance x_m on the actual surface. The velocity profile within the boundary layer at x_m ($\overline{x_m}$) is assumed to be described as the power law that is:

$$\frac{u}{V_e} = \left(\frac{y}{\delta}\right)^{\frac{1}{n}}$$

The Stratford criterion for a locating the separation point x, is expressed by:

$$\left(2\overline{Cp}\right)_s^{(n-2)/4}\left(x\frac{d\,\overline{Cp}}{d\,x}\right)_s^{1/2} = N\beta\left(10^{-6}\overline{\mathrm{Re}}\right)^{1/10} \tag{3.3}$$

where

$$\overline{Cp} = \frac{p - p_m}{q_m}$$

$$\overline{\mathrm{Re}} = \frac{U_m\,\overline{x_m}}{\nu}$$

$$N = 11.36\frac{(n-2)^{(n-2)/4}}{(n+1)^{(n+1)/4}(n+2)^{1/2}}$$

The subscript m and s denote values at the point of the maximum velocity and the point of separation respectively, and β is a function of the shape of the pressure distribution in

the region near separation. Since the range 6<n<8 covers most applications, with n=6, the criterion above takes the form:

$$S(x) = \left[\frac{\overline{Cp}\left(\overline{x} \frac{d\overline{Cp}}{dx} \right)^{1/2}}{\left(10^{-6}\overline{\mathrm{Re}}\right)^{1/10}} \right] \tag{3.4}$$

where

$$S = \begin{cases} 0.35 & for \quad \dfrac{d^2 p}{dx^2} \le 0 \\ 0.39 & for \quad \dfrac{d^2 p}{dx^2} > 0 \end{cases}$$

As the equality represented above is valid only at the separation point, calculated at each point over the surface from the point where the boundary layer started, when S reaches the criterion in terms of S, separation is assumed to exist.

The calculation of x_s for a specific pressure distribution and given location of laminar-turbulent transition x_t is facilitated by use of the approximate formula below [1]:

$$\overline{x_m} = 38.2 \left(\frac{\nu}{u_t x_t} \right)^{3/8} \left[\int_0^1 \left(\frac{V_e}{u_t} \right)^5 d\left(\frac{x}{x_t} \right) \right]^{5/8} + \int_{x_i}^{x_m} \left(\frac{V_e}{u_m} \right)^3 dx \tag{3.5}$$

Since x_m is known and $\overline{x_s}$ - $\overline{x_m}$ = $x_s - x_m$ where $\overline{x_s}$ and $\overline{x_m}$ are given, the predicted separation distance, x_s , is

$$x_s = x_m + (\overline{x_s} - \overline{x_m}) \tag{3.6}$$

Prediction computation based on Stratford's method has been done by the program 'predictx.for'. This program as well as the others requires the input data file

'cps.dat' and put the calculated results into the output data file, names of which vary one program from another while all programs use the same name for their input data files, which as shown above is 'cps.dat'. This is done only for convenience. Throughout my research, separation on the upper, or suction, side surface is mainly focused on. This is mainly because unlike the upper side case, over a certain value of the angle of attack, the location of separation on the lower side surface will rapidly moves toward the trailing edge and then hardly moves. Therefore, once the code starts running, it at first searches for the leading edge stagnation point and having that point as the starting point, the code calculate whatever data necessary for each computation method over the upper surface from the leading edge stagnation point to the trailing edge. This 'the leading edge-the trailing edge over the upper surface' procedure can be seen every computer code used in the current research.

3.2.2 Goldschmied's method

Like Stratford's method, Goldschmied's method [5] is a single parameter method and can be considered even simpler than Stratford's method. Once the skin friction coefficient at the point of maximum velocity is obtained, it doesn't require any calculation on the pressure distribution, which is given at the first place. The program simply looks for the point where the value of Cp is 200 times as large as C_{fm}. The advantage of this method is, of course, its simplicity. On the other hand, the

disadvantage is that this method is somewhat inconclusive. Goldschmied's method tends to predict both 'early' and 'late' separation. This is probably as a result of the very questionable assumption concerning the total pressure at the edge of the viscous sub layer.

Goldschmied's method is the method relating the maximum pressure recovery ratio at the separation point to the skin friction coefficient at the start of the adverse gradient. The criterion used in this method for locating the point of separation cannot be more simple and is expressed as

$$C_{psep} = 200C_{fm} \tag{3.7}$$

So that separation is assumed to happen where the local pressure coefficient, Cp, reaches the value of $C_{fm} \times 200$. The theory on which this prediction method is built depends on the assumption of the dissipate-region similarity under any pressure gradient and of the existence of a constant total-head line at a fixed distance from the wall under adverse pressure gradient. Generally employing the momentum integral equation, eq.(3.8), and using H (shape factor) as a separation criteria, most of the separation prediction methods for incompressible turbulent flow are too laborious for hydrodynamic (airfoil) designer. Goldschmied's method was developed for the predicting separation point in incompressible two dimensional turbulent boundary layer with adverse pressure gradient. The method is mainly depending on two characteristics of the boundary layer , which are the existence of the dissipative region within the boundary layer and of the constant total-head line. Townsend pointed out that the boundary layer can be divided into three regions with respect to the energy flow [5].

1. The mixing (the outer) region

The region where the energy flow from the freestream line is captured.

2. The energy transfer (the middle) region

The region where the energy flow of turbulent energy is directed toward the wall.

3. The dissipative (the inner) region

The region where all the energy flow is absorbed and dissipated.

And in the dissipative region, only very close to the wall, there is a similarity of the velocity profile independent of the pressure gradient. It is obvious by definition that the total head remains constant in the freestream at very large distant from the wall and, on the other hand, at the wall the static pressure increases with 'adverse pressure gradient'. Also it is well known that within the boundary layer at comparatively large distance from the wall, the total head decreases. What is not generally recognized is the fact that within the boundary layer at small distance from the wall, there is a region where the total head increases. This may seem strange, however, the concept of the dissipative layer receiving the energy flow follows this idea of the total-head increasing region.

In addition, some experiment indicate that such increasing total-head lines are independent of the pressure gradient at least when adverse pressure is not too high.

If useful results can be achieved, it is permissible to make the simple assumption, which is that there is a line in the dissipative region at constant distance from the wall along which the total-head is exactly constant. Accepting this assumption, and let us follow the process to obtain the simple criterion of this method. Suppose there is a line in the inner region at a constant distance from the wall, with a constant, such that

$$h_c = p + \frac{1}{2}\rho u_c^2$$

It is known that the outer edge of the inner region is approximately characterized

$$\frac{u}{u^*} = 20$$

$$\frac{y\,u^*}{\nu} = 500$$

Then the total head at the start of the adverse pressure gradient can be written as

$$h_m = p + \frac{1}{2}\rho u_m^2$$

$$= p + \frac{1}{2}\rho\left(20u_m^*\right)^2$$

where the subscript m denotes the value at the point of the maximum velocity. Taking the constant-total head line at the maximum velocity point as the starting point of calculation, from that point the relation below is always assumed to be true.

$$h_c = p_m + \frac{1}{2}\rho\left(20\,u_m^*\right)^2$$

$$p + \frac{1}{2}u_c = p_m + \frac{1}{2}\rho\left(20\,u_m^*\right)^2$$

then,

$$p_m - p + \frac{1}{2}\left(400\left(\frac{\tau_w}{\rho}\right)\right) = \frac{1}{2}\rho\,u_c$$

$$\frac{2(p_m - p)}{\rho} + 400\left(\frac{\tau_w}{\rho}\right) = u_c^2$$

$$\left(\frac{u_c}{u_m}\right)^2 = \frac{p_m - p}{\frac{1}{2}\rho\,u_m^2} + 400\left(\frac{\tau_w}{\rho\,u_m^2}\right)$$

so that

$$\left(\frac{u_c}{u_m}\right) = \left(200\, c_{fm} - C_p\right)^{\frac{1}{2}}$$

Making use of the laminar sublayer and the law of the wall,

$$\frac{u_c}{u_m} \approx 0 \qquad \text{at the point of separation}$$

therefore, where separation occurs,

$$Cp_{sep} = 200 c_{fm} \tag{3.7}$$

As the line is in the dissipative region, this assumption is independent of pressure gradient. It is logical to assume that this line is expected to be along the outer edge of the dissipative region. This assumption concerning the constant total-head line is, of course, not exactly true. The characteristics of the dissipative region mentioned above is not exactly independent of the pressure gradient and second, at constant distance from the wall, the total-head, actually, is both increasing and decreasing, depending on the place one is looking at. So that there cannot be a line of substantially constant total-head.

3.2.3 Thwaites's Method

Thwaites's method here and Head's method to be explained in the following section are implemented into one program named 'integrl4.for'. In this program, Thwaites's method is responsible for the laminar boundary layer calculation. In other

words, the boundary layer solutions are continuously calculated at each point along the airfoil surface up to the transition point, then after that point Head's method takes over the calculation. By integral-type method, meaning that momentum integral equation is solved, the point of separation can be predicted with high accuracy. Main disadvantage, however, is that methods of this type are so complicated and laborious that it is not easy to code them.

Thwaites's method is the momentum integral method for the laminar boundary layer. The method is to supplement the momentum integral equation below

$$\frac{d\theta}{dx}+\frac{\theta}{V_e}(2+H)\frac{dV_e}{dx}=\frac{1}{2}c_f \tag{3.8}$$

with algebraic relation among the unknowns θ, H, and c_f . Introducing the parameter,

$$l\equiv\frac{\rho V_e\theta}{2\mu}c_f \qquad \left(\equiv\frac{1}{2}\mathrm{Re}_\theta\, c_f\right) \qquad \mathrm{Re}_\theta=\frac{\rho V_e\theta}{\mu} \tag{3.9}$$

the momentum integral equation is multiplied by Re_θ to get:

$$\frac{\rho V_e\theta}{\mu}\frac{d\theta}{dx}+\frac{\rho\theta^2}{\mu}(2+H)\frac{dV_e}{dx}=l \tag{3.10}$$

Thwaites defined a dimensionless pressure-gradient parameter,

$$\lambda\equiv\frac{\rho\theta^2}{\mu}\frac{dV_e}{dx} \tag{3.11}$$

and the above equation (3.9) can be rewritten

$$\frac{\rho V_e}{\mu}\frac{d^2\theta}{dx^2} = 2\left[l-(2+H)\lambda\right] \tag{3.12}$$

Thwaites found that the right side of eq.(3.11) can be well approximated by the simple formula,

$$2\left[l-(2+H)\lambda\right] \approx 0.45 - 6\lambda \tag{3.13}$$

From eq.(3.11) and eq.(3.12),

$$\frac{\rho V_e}{\mu}\frac{d^2\theta}{dx^2} = 0.45 - 6\lambda \tag{3.14}$$

Substituting the definition of λ, eq.(3.10),

$$\frac{\rho V_e}{\mu}\frac{d^2\theta}{dx^2} = 0.45 - \frac{6\rho\theta^2}{\mu}\frac{dV_e}{dx} \tag{3.15}$$

Moving the dVe/dx term to the left side and multiplying by V_e^5,

$$\begin{aligned}&\frac{\rho}{\mu}\left(V_e^6\frac{d\theta}{dx} + 6\theta^2 V_e^5\frac{dV_e}{dx}\right)\\ &= \frac{\rho}{\mu}\frac{d}{dx}\left(\theta^2 V_e^6\right) = 0.45V_e^5\end{aligned} \tag{3.16}$$

Then:

$$\frac{d}{dx}\left(\theta^2 V_e^6\right) = 0.45\nu\, V_e^5 \tag{3.17}$$

$$\theta^2 V_e^6 = 0.45\nu\int_0^x V_e^5 dx \tag{3.18}$$

$$\theta^2 = 0.45\frac{\nu}{V_e^6}\int_0^x V_e^5 dx \tag{3.19}$$

Thus, on given Ve(x) and the initial value of θ(0), θ(x) can be determined by eq.(3.18), which is a really simple task. Once θ is obtained, λ can be calculated from eq.(3.11)

and then l (λ) and H(λ) are given by correlation formulas [12]:

$$\begin{aligned} l(\lambda) &= 0.22 + 1.57\lambda - 1.8\lambda^2 && 0 < \lambda < 0.1 \\ &= 0.22 + 1.402\lambda + \frac{0.018\lambda}{\lambda + 0.107} && -0.1 < \lambda < 0 \end{aligned} \tag{3.20}$$

$$\begin{aligned} H(\lambda) &= 2.61 - 3.75\lambda + 5.24\lambda^2 && 0 < \lambda < 0.1 \\ &= 2.088 + \frac{0.0731}{\lambda + 0.14} && -0.1 < \lambda < 0 \end{aligned} \tag{3.21}$$

In Thwaites's method the condition c_f, then l =0, is used as separation criterion. When l =0, or λ= -0.0842 which makes l =0, the flow is assumed to separate. Since this method includes the first-order ordinary differential equation eq.(3.17), one initial condition is needed. One can easily imagine two typical cases, one is the boundary layer with zero starting thickness as found in the case of a flat plate, and the other one is Non-zero initial momentum thickness as seen in the case the flow past an airfoil, which is the case of my research. For the boundary layer with non-zero initial thickness from its start at the stagnation point, the starting momentum thickness can reasonably be assumed as:

$$\theta = \sqrt{\frac{0.075\mu}{\rho \left.\frac{dV_e}{dx}\right|_{x=0}}} \qquad \text{at the leading edge stagnation point [12]} \tag{3.1}$$

3.2.4 Head's Method

Head's Method is for the turbulent boundary layer and based on the concept of an entrainment velocity. If δ(x) is the boundary layer thickness, the volume rate of flow within the boundary layer at x is:

$$Q(x) = \int_0^{\delta(x)} u\,dy \tag{3.22}$$

The entrainment velocity E is defined as the rate at which Q increases with x

$$E = \frac{dQ}{dx} \tag{3.23}$$

The idea as to the physical significance of E can be described as shown below,

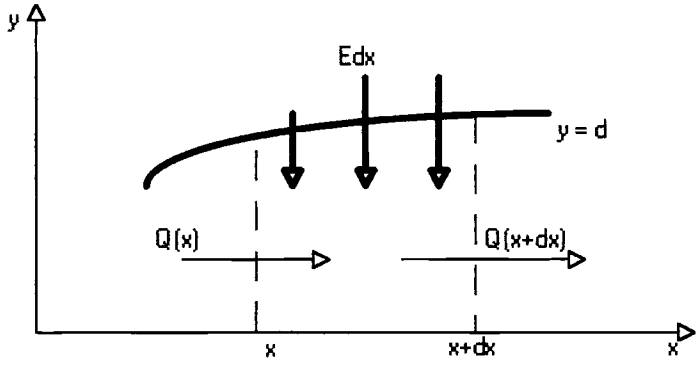

Figure 3.2. Concept of entrainment [10]

From eq.(3.22) and the definition of the displacement thickness shown below,

$$\delta^*(x) \equiv \int_0^{\infty} \left[1 - \frac{u(x,y)}{V_e}\right] dy \tag{3.24}$$

and

$$\delta^* = \delta - \frac{Q}{V_e}$$

then

$$Q = V_e(\delta - \delta^*)$$

$$E = \frac{d}{dx} V_e(\delta - \delta^*)$$

The last equation (3.23) can be rewritten as

$$E = \frac{d}{dx}(V_e \, \theta \, H_1) \tag{3.25}$$

where

$$H_1 \equiv \frac{\delta - \delta^*}{\theta} \tag{3.26}$$

It is assumed by Head that the dimensionless entrainment velocity E/Ve depends only on H_1 and that H_1, in turn, is a function of $H = \delta^*/\theta$ as follows:

$$\frac{1}{V_e}\frac{d}{dx}(V_e \, \theta \, H_1) = 0.0306(H_1 - 3)^{-0.6169} \tag{3.27}$$

$$\begin{aligned} H_1 &= 3.3 + 0.8234(H - 1.1)^{-1.287} \quad for \quad H \geq 1.6 \\ &= 3.3 + 1.5501(H - 0.6778)^{-3.064} \quad for \quad H > 1.6 \end{aligned} \tag{3.28}$$

These two equations and the momentum integral equation shown below

$$\frac{d\theta}{dx} + \frac{\theta}{V_e}(2 + H)\frac{dV_e}{dx} = \frac{1}{2}c_f \tag{3.29}$$

$$H \equiv \frac{\delta^*}{\theta}$$

represent three questions among the four unknown θ, H, H_1 and c_f.

Head added the fourth required equation to complete the solution, which is Ludwieg-Tillman skin friction "Law"

$$c_f = 0.246 \times 10^{-0.678H} \, \mathrm{Re}^{-0.268} \tag{3.30}$$

Like most integral methods, this method uses the shape factor, H, as the separation criterion. When H is in the range 1.8 to 2.4, separation is assumed to occur and in my program H = 2.4 is taken as the criterion. Since as flow gets close to the point of separation, the shape factor increases so quickly that the difference between the lower and upper limits of H hardly matters. In the program developed for the current study, after using Thwaites's method to calculate the growth of the laminar separation up to the transition point, program switches the method and begin to calculate for the turbulent boundary layer region. Following the laminar boundary layer growth up to the point of transition, Thwaites's method can provide the boundary layer data on θ, H and c_f. However, H and c_f changes so dramatically during transition that only the resultant value of θ can be used as the starting value for the turbulent boundary layer region. To get the initial value of H for the turbulent boundary layer region, Moran [12] suggests one just guesses the starting value of H as is found the shape factor for a turbulent boundary layer usually in a rather narrow range. In a mild pressure gradient, it takes the value of 1.3 to 1.4. With fixed transition option switch on, the transition to turbulent is fixed at the point of the maximum velocity over the surface, which is expected to be, and actually, very close to the leading edge. Therefore, unlike it is stated above, the pressure gradient near the leading edge is not 'mild' enough to expect the starting value of H for the turbulent boundary layer to lie in the range 1.3-1.4. With the starting value of H = 1.5 for the current study, instead of 1.3-1.5, the calculated results have a good agreement with the experimental data, which is shown later.

3.3 The Effect of The Boundary Layer Separation on Aerodynamic Characteristics

As mentioned many times before, the boundary layer separation does have a great effect on the aerodynamic characteristics of an airfoil. The aerodynamic load of an airfoil experiencing flow separation differs from that of an airfoil with no separation so that the values of the aerodynamic characteristics should be corrected to take into account the effect of separation on an airfoil. If a separation of length S_{sep} on the upper surface measured over the surface from the trailing edge is obtained by a separation prediction method, c_l can be corrected [15] by:

$$\begin{aligned} \Delta c_l &= 2\pi \Delta\alpha \\ \Delta\alpha &= -\frac{S_{sep}}{2c}\left(\delta_{us} + \alpha_c\right) \end{aligned} \tag{3.31}$$

where δ_{us} is the angle measured at the trailing edge between the upper surface and the chord line, and α_c is the angle of attack measured at the trailing edge as well. The moment coefficient c_m is corrected correspondingly. The correction of moment is made as [15]:

$$\Delta c_m = -\frac{1}{4}\Delta c_l\left(1-\frac{S_{serp}}{c}\right)^{1.5} \tag{3.32}$$

The corrections on the lower surface can be made in the same way. In my computation, however, the effect of separation on the lower surface side is excluded as separation on the upper side has a much stronger effect on the aerodynamic load of an airfoil. In addition to this, unlike the location of separation on the upper, or suction, side, the point of separation on the lower, or pressure, side is known to tend to move toward the trailing

edge as the angle of attack increases. Therefore, its effect on the aerodynamic characteristics is nothing much to consider.

3.4 Computer Code

3.4.1 Stratford's method code

The code 'predictx.for' has been developed to calculate the point of separation with given pressure distribution by Stratford's method. This program reads input file 'cps.dat' and write the calculated results into output file 'strat.dat'. The code first reads the input file and find the leading edge stagnation point. Then, the code reorders the input data and the leading edge stagnation point becomes the first point to be processed. After that calculation continues at each point to the trailing edge over the upper surface.

The point of transition is assumed to be at the point where the velocity gets its maximum value, and the transition point is fixed there. Stratford's coefficient is to be calculated after the transition point, then to be written into the output file 'strat.dat'. Once the code reaches the trailing edge, it is terminated.

Now, one can open the output file and look for the point where Stratford's coefficient reaches a certain value shown below [1], Stratford's criterion, and the possible separation can be detected.

$$S = \begin{cases} 0.35 & for \quad \dfrac{d^2 p}{d x^2} \le 0 \\ 0.39 & for \quad \dfrac{d^2 p}{d x^2} > 0 \end{cases}$$

Seen in the potential flow-based chordwise pressure distribution, in most cases $\frac{d^2 p}{d x^2} > 0$, and therefore, S=0.39 was supposed to be a criterion. However, as mentioned by Cebeci [19], it was observed that Stratford's method has better agreement with experiment if the criterion value was slightly changed to 0.5. This is also true in the current study, therefore, $S_{sep} = 0.5$ was used to predict the separation.

The program has been run on PC, and for any case the run-time is no more than one second.

3.4.2 Goldschmied's method code

The code 'goldx.for' has been developed to calculate the point of separation with given pressure distribution by Goldschmied's method. This program reads input file 'cps.dat' and write the calculated results into output file 'gold.dat'. The code first reads the input file and find the leading edge stagnation point. Then, the code reorders the input data and the leading edge stagnation point becomes the first point to be processed. After that calculation continues at each point to the trailing edge over the upper surface.

The point of transition is assumed to be fixed at the point where the velocity gets its maximum value.

This method is the method relating the maximum pressure recovery ratio at the separation point to the skin friction coefficient at the start of the adverse gradient. The criterion based on this concept is shown below

$$C_{psep} = 200\, C_{fm} \tag{3.7}$$

and accordingly, the point where the local Cp reaches the value of $C_{fm} \times 200$ will be assumed to be the separation point.

Consequently, C_{fm} should be known in advance. Taking advantage of the concept on which Stratford's method is based, the value of C_{fm} was deduced as follows. The boundary layer can be characterized by θ, and based on this fact, Stratford's method calculates 'equivalent' constant pressure region from actual pressure distribution. Then, the designated 'equivalent constant pressure' region is to be used, instead of 'actual' pressure distribution. No matter which pressure feature the flow within the boundary layer is coming through, at the start of the adverse pressure distribution, the state of the resultant boundary layer can be considered identical. Thus, C_{fm} can be calculated by making use of the fact regarding this 'equivalent' pressure region and another fact that in such a region, a equivalent to 'flat' plate region, C_f can be calculated as [6]:

$$C_f \cong \frac{0.73}{\sqrt{\mathrm{Re}_x}} \qquad \text{for the laminar boundary layer} \tag{3.33}$$

Once C_f is obtained, the following procedure is hardly complicated and even doesn't require any calculation. Looking for the point on the surface of the airfoil where the value of Cp is equal to or more than $C_{fm} \times 200$, the point of separation is to be found.

3.4.3 Integral method code

The code 'intgrl4.for' has been developed to predict the location of separation by Thwaites-Head integral-type combined method.

After the code starts running, it asks you to input what transition point criterion to use and the Reynolds number. Three transient criterion options are available, Michel criterion, the maximum velocity point and the manually fixed point. If 'manually fixed' option is selected, the code also asks where to put the transition point. If one selected this option and input '3', then the third point after the leading edge stagnation point is to be the point of transition.

Finally, the code is ready to start the boundary layer calculations. First, Thwaites's method for the laminar boundary layer region is employed up to the transient point. Thwaites's method is used until one of three things below happens:

- The code detects the trailing edge
- Laminar separation is detected. This is when the value of λ becomes less than -0.0842.

- Transition set by one of three transition options is detected.

In the last case, Head's method for the turbulent boundary layer takes over the calculations. It begins by asking for the value of H at transition. Moran [12] mentioned that the response should be in the range 1.3 to 1.4, however, as shown later, when potential flow solutions are dealt with, the current study indicates H=1.5 is appropriate for reasonable results for airfoils examined here.

The calculation proceeds until turbulent separation is predicted, or the trailing edge is reached. Here, the criterion for turbulent separation is based on the computed value of H, which is to be displayed on screen, and when H reaches 2.4, the code declares that the turbulent boundary layer has separated.

CHAPTER IV

RESULTS

4.1 The sharp pressure spike near the leading edge.

The steep pressure drop seen in potential flow solutions is the initial motivation to this survey. Since this phenomenon known as the leading edge suction is also seen in experimental data to some extent, as long as the angle of attack is small enough, the pressure distribution obtained experimentally is hardly different from that calculated by potential flow theory.

In airfoil potential flow solutions, however, as the angle of attack gets larger, this pressure spike can grow to unrealistically large extent and becomes dominant to entire chord-wise pressure distribution on an airfoil. This causes the pressure distribution obtained from potential flow theory to be different from that seen in experimental data. The difference could be negligible where the angle of attack is small enough, but as the angle of attack gets larger, this difference in the pressure distribution comes to make a significant difference on the resulting aerodynamic characteristics of an airfoil by experiment and by potential flow theory.

The chord-wise distribution for NACA4412 with varied angle of attack is shown here in Figure 4.1-3. As mentioned above, the steep pressure spike is noticeable, as the angle of attack becomes larger. Notice that even for the angle of attack of 8°, the pressure distribution obtained from potential flow solutions can hardly be close to that seen in experimental data. After that, it is easy to see that the larger the angle of attack becomes, the more difference can be seen in the comparison. Also, it is worth noting that there is the peak value of the minimum Cp in experimental data while the minimum value of Cp is simply getting lower in the potential flow solutions.

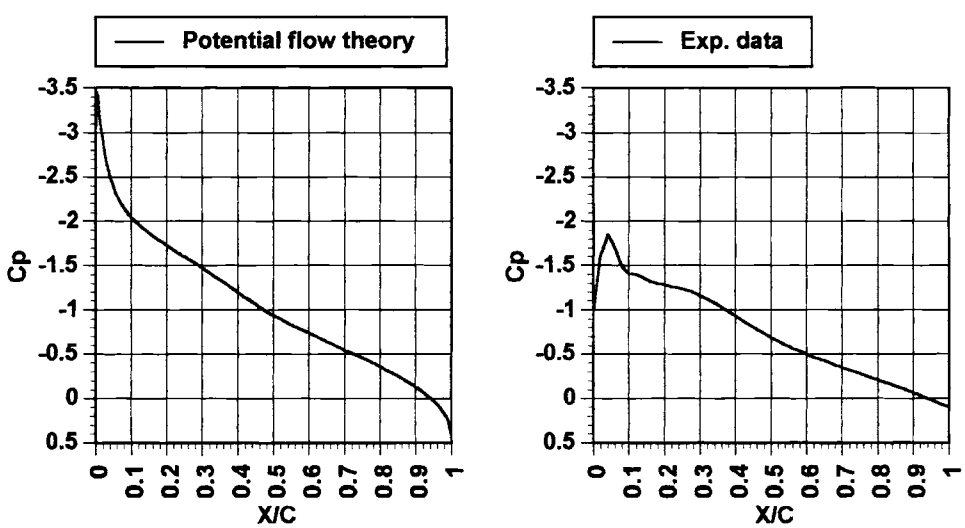

Figure 4.1. The chord-wise pressure distributions obtained by potential flow calculation and observed in experimental data [19]. (NACA4412, α=8°, Re=3,000,000)

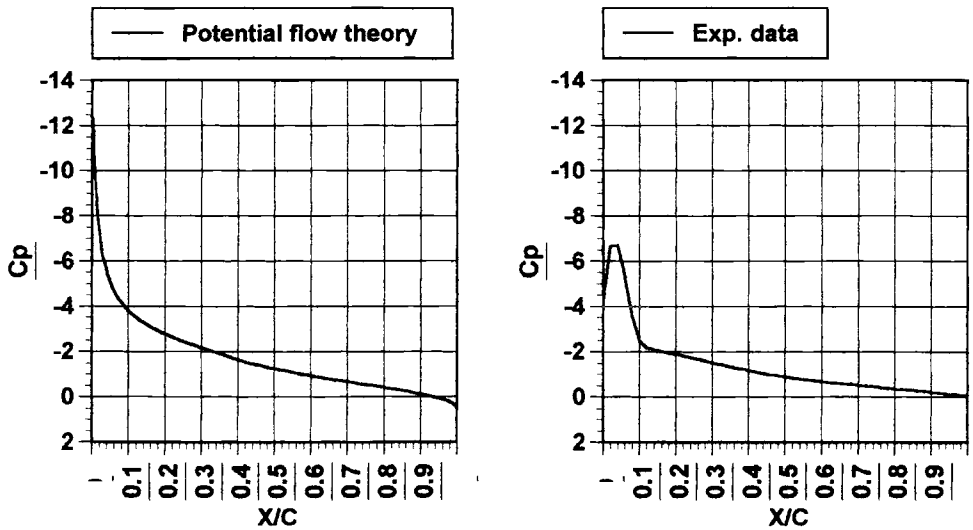

Figure 4.2. The chord-wise pressure distributions obtained by potential flow calculation and observed in experimental data [19]. (NACA4412, α=16°, Re=3,000,000)

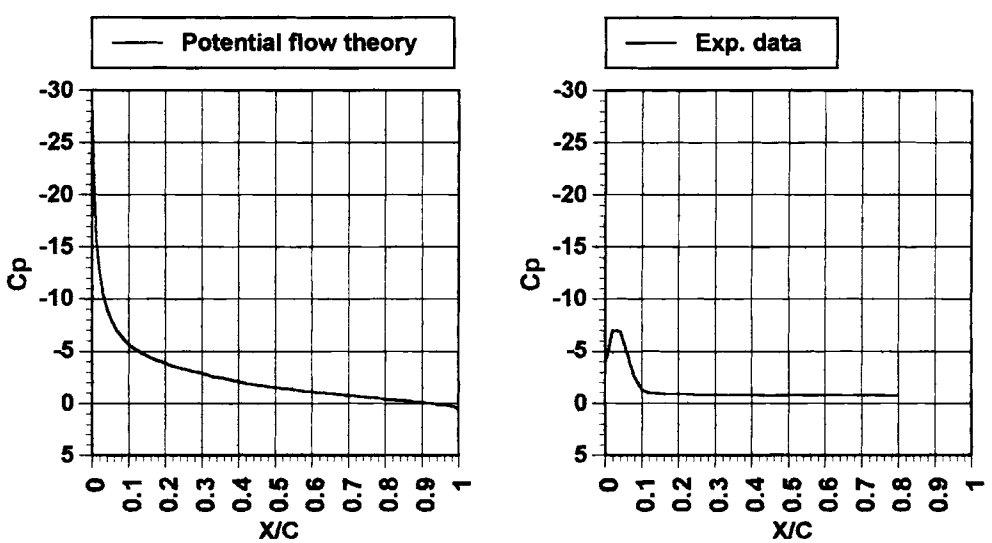

Figure 4.3. The chord-wise pressure distributions obtained by potential flow calculation and observed in experimental data [19]. (NACA4412, α=8°, Re=3,000,000)

The minimum value of Cp is found at the angle of attack of 20° in experimental data as to NACA4412 with $Re=3\times10^6$, and then the minimum value of Cp is, indeed, getting larger as the angle of attack becomes larger, which is not the case of potential flow solutions.

4.2 Code validation where the angle of attack is small.

4.2.1 Stratford's method code validation with the small angle of attack.

Stratford's method is one of the simplest methods, which uses only the pressure distribution to predict the boundary layer separation. It doesn't require detailed boundary layer calculation like integral-type methods to be discussed later. Because of its simplicity it is easy to code Stratford's method so that this prediction method was chosen at the first place.

The points of separation have been calculated with the pressure distribution based on potential flow solutions, not experimental data, and the results are seen in Figure 4.4, where NACA4412, NACA0012 were used.

In the range of the angle of attack 0° to 7° shown in these figures, the location of separation is expected to be the at the trailing edge, or X/C=1. Considering the nature of Stratford's method tending to predict early separation, in this range of the angle of attack,

it is reasonable to say that Stratford's method can be applied to potential flow solutions and still used as a tool to estimate the characteristics of separation of an airfoil.

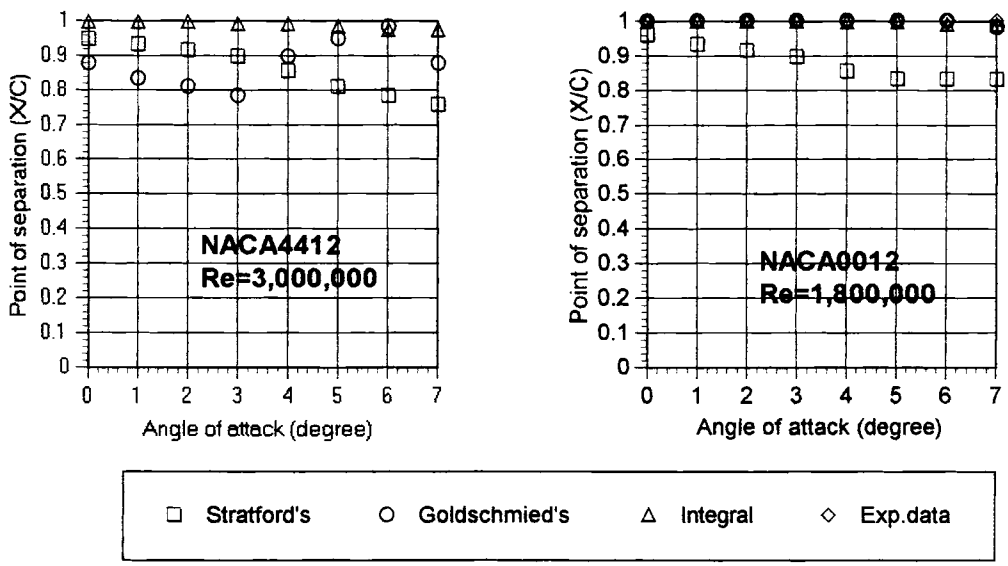

Figure 4.4. Calculated separation point with small angle of attack 0°-7°
Exp.data from [20]

4.2.2 Goldschmied's method

Like Stratford's method this method is a single parameter method and doesn't require detailed boundary layer solutions. By observing Figure 4.4, the same conclusion as the case of Stratford's method can be deduced. In the range of the angle of attack of 0° to 7°, the resulting point of separation remain close to the trailing edge while experimental data indicates X/C≈1, in this region of the angle of attack.

4.2.3 Integral method (Thwaites's - Head's combined method)

After two simple methods mentioned above, the integral method indicated the most accurate results. While separation is hardly expected in this range of small angle of attack, therefore X/C≈1 can be seen in experimental data, the calculated points of separation is located at 1-0.95 in terms of X/C. This resultant separation point by Integral method is very consistent with the data obtained by experiment in the range of the angle of attack. Notice that as seen in Figure 4.1, even at the angle of attack of 8°, the difference in the chord-wise pressure distribution between by experiment and by potential flow solutions is so easy to notice that at α=7°, the pressure difference is also expected to be different to nearly the same extent. However, in spite of this, Integral method seems to capture the separation characteristics seen in experimental data surprisingly well.

4.3 The region of high angle of attack

How each method works where α is large, larger than 7°, has been examined and the results can be seen in Figure 4.5-6. Recall that where α is this large, the magnitude of the pressure spike at the leading edge in potential flow solutions becomes significantly

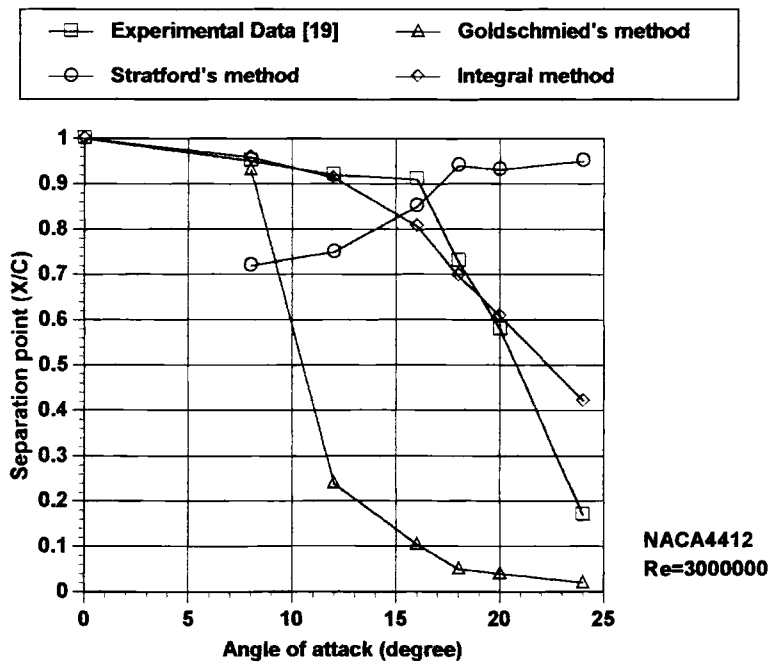

Figure 4.5. Calculated characteristics of separation with high angle of attack on NACA4412

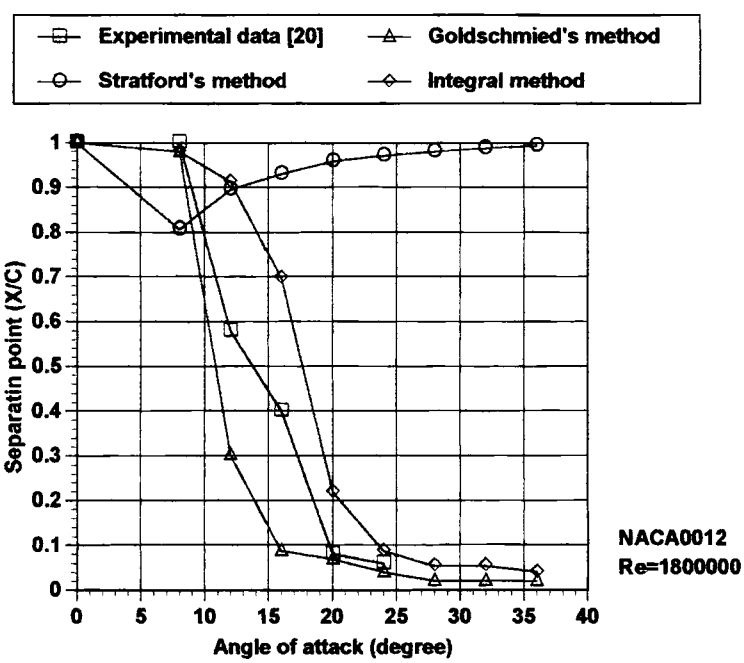

Figure 4.6. Calculated characteristics of separation with high angle of attack on NACA0012

large, and consequently, the pressure distribution expected by potential flow theory comes to be totally different from that obtained by experiment. This is, indeed, seen in Figure 4.1-3.

As expected, the two simple methods break down here. In both Figure 4.5-6, the points of separation predicted by Stratford's method move toward the trailing edge as αbecomes lager, which is totally contradictory to intuition as well as experimental data.

The way Stratford's method breaks down as α gets larger is possibly related to the form of the formula of Stratford coefficient, eq (3.4) and shown below as well, and can be analyzed as follows:

$$S(x) = \left[\frac{\overline{Cp}\left(x \frac{d\overline{Cp}}{dx} \right)^{1/2}}{\left(10^{-6}\overline{\mathrm{Re}}\right)^{1/10}} \right] \tag{3.4}$$

Where α is large, the potential theory-based pressure distribution comes to considerably differ from the experimental data. The magnitude of sharp pressure drop seen near the leading edge becomes large. This causes $\overline{\mathrm{Re}}$ in eq.(3.4) to be much larger than it actually is in a real flow.

Now observe Stratford formula, eq.(3.4). Even though the magnitude of Cp, or $\overline{C_p}$ can become very large in potential flow theory, this large magnitude occurs very close to the leading edge where $\bar{x}$ is very small so that as a whole the numerator of eq.(3.4) remains small enough not to meet the Stratford's separation criterion. In

addition, large $\overline{\mathrm{Re}}$, which makes the denominator of eq.(3.4) large, also helps Stratford's coefficient to remain small.

Further down stream, the magnitude of pressure drop becomes nearly the same between experimental data and potential-based pressure distribution. However, much larger $\overline{\mathrm{Re}}$ seen in potential flow makes the denominator of eq.(3.4) larger and keeps S(x) from meeting the Stratford criterion.

In this way, when applied to potential flow solutions, Stratford's method always predicts the point of separation near the trailing edge regardless of α. Moreover, the larger the α is , the further back the point of separation moves.

On the other hand, Goldschmied's method seems to predict 'too' early or conservative separation point on NACA4412 while the method work relatively well on NACA0012.

Observing eq.(3.7) on which Goldschmied's method based and how C_{fm} is obtained, this tendency of 'too' early separation can be explained as follows.

$$C_{psep} = 200 C_{fm} \tag{3.7}$$

Taking advantage of Stratford's method, the C_{fm} is calculated [6] as

$$C_f \cong \frac{0.73}{\sqrt{\mathrm{Re}}} \tag{3.33}$$

Seen in Figure 4.1-3, as the α is larger, the maximum velocity to be achieved becomes larger, and therefore, $\overline{\mathrm{Re}}$ gets larger as well. Thus, observing eq.(3.33), the larger α is, the smaller the value of C_f becomes. Consequently the separation criterion will be easier to be met as α is getting larger. So where α is large enough, there will be 'too' early separation to be predicted through Goldschmied's method.

Notice that surprisingly, the results by Integral method have an excellent agreement with experimental data on both NACA0012 and NACA4412. Additionally it is worth noting that despite the difference in the pressure distribution between experimental data and data based on potential flow solutions caused by the existence of the 'steep' pressure spike seen in potential flow solutions, Integral method still seem to be able to cancel out the effect of the sharp pressure spike and keep capturing the characteristics of separation of an airfoil.

It is worth noting that as seen in Figure 4.1-3, although the sharp pressure drop, which is contrary to experimental data, is seen near the leading edge in potential flow-based pressure distribution, further downstream, the pressure distribution by potential theory is nearly identical to that by experiment. In other words, the steep pressure spike characterizing the potential flow-based pressure distribution is confined within the limited and narrow region very close to the leading edge.

Again, the steep pressure spike is occurring in the very narrow region in terms of x. Using integral-type prediction methods, the effect of the steep spike to the separation prediction can be weakened in the process of integrating boundary solutions in x direction. Consequently, dealing with potential flow-based pressure distribution by integral method becomes almost equivalent to dealing with real pressure distribution. As a result, the point of separation calculated by integral-type method with potential flow-based pressure distribution is much closer to that seen in experimental data, and one can capture the separation characteristics seen in experimental data by calculation based on potential flow-based pressure distribution.

4.4 Corrected Cl, Cm by Integral method.

Integral method's validity when applied to potential flow solutions has been seen in the preceding section. In this section, the aerodynamic characteristics, Cl and Cm, of an airfoil obtained from potential flow solutions is discussed, and then, the correction has been made on them making use of equations shown below [15].

$$\Delta c_l = 2\pi \Delta\alpha$$
$$\Delta\alpha = -\frac{S_{sep}}{2c}(\delta_{us} + \alpha_c) \tag{3.31}$$

$$\Delta c_m = -\frac{1}{4}\Delta c_l\left(1 - \frac{S_{serp}}{c}\right)^{1.5} \tag{3.32}$$

When separation occurs on the upper surface, the lift coefficient c_l is corrected by changing the effective angle of attack in a way which is derived from Helmholtz Theory [15]. So, eq.(3.31) was obtained.

The moment coefficient c_m is corrected as follows. As a result of separation and c_m is changed. When the boundary layer separates near the trailing edge, the same effect can be achieved by assuming a flap deflected. The length of the flap is approximately S_{sep} in this case. The effect of such a flap on the moment can be calculated by linearlized theory , and eq.(3.32) was obtained.

The resulting aerodynamic characteristics and comparison with experimental data can be seen in Figure 4.7-13. The different kinds of NACA airfoil series have been selected and examined to see how the potential flow-based aerodynamic characteristics captures the experimental data qualitatively.

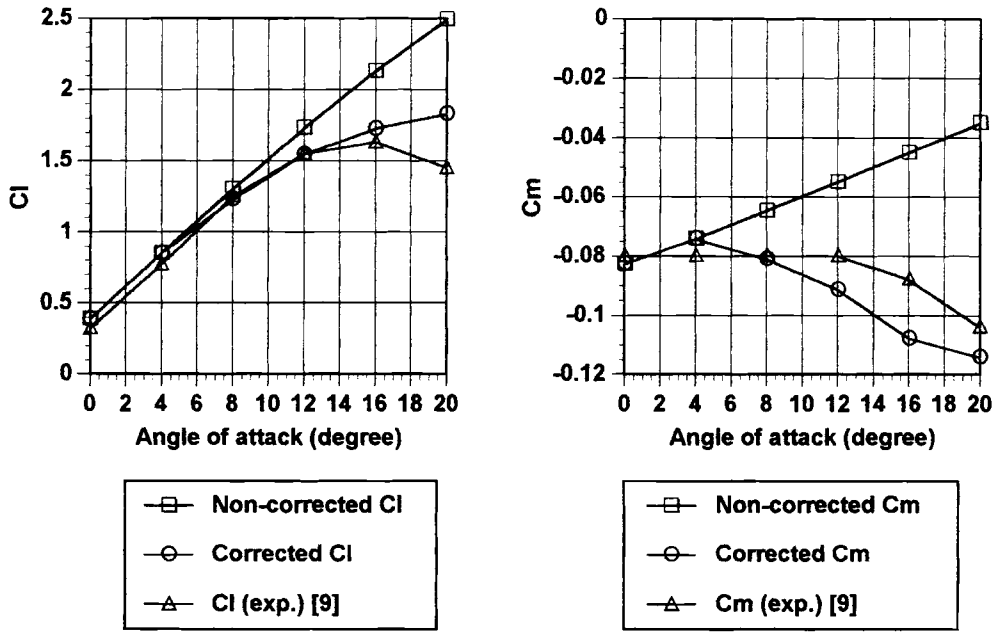

Figure 4.7. Corrected Cl, Cm on NACA747A315, Re=6,000,000

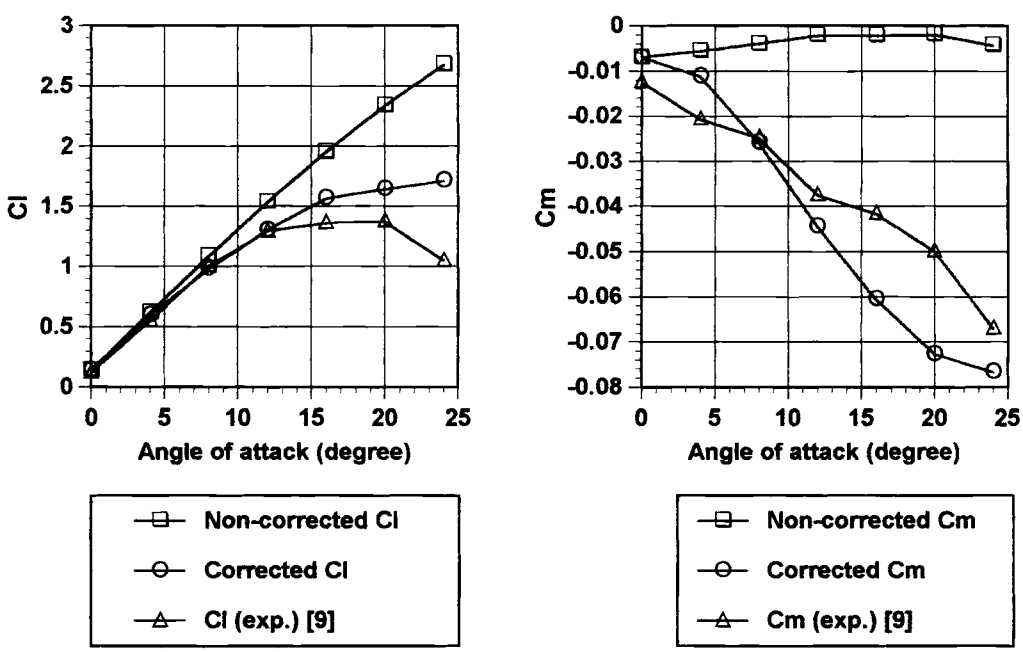

Figure 4.8. Corrected Cl, Cm on NACA63$_2$-415, Re=6,000,000

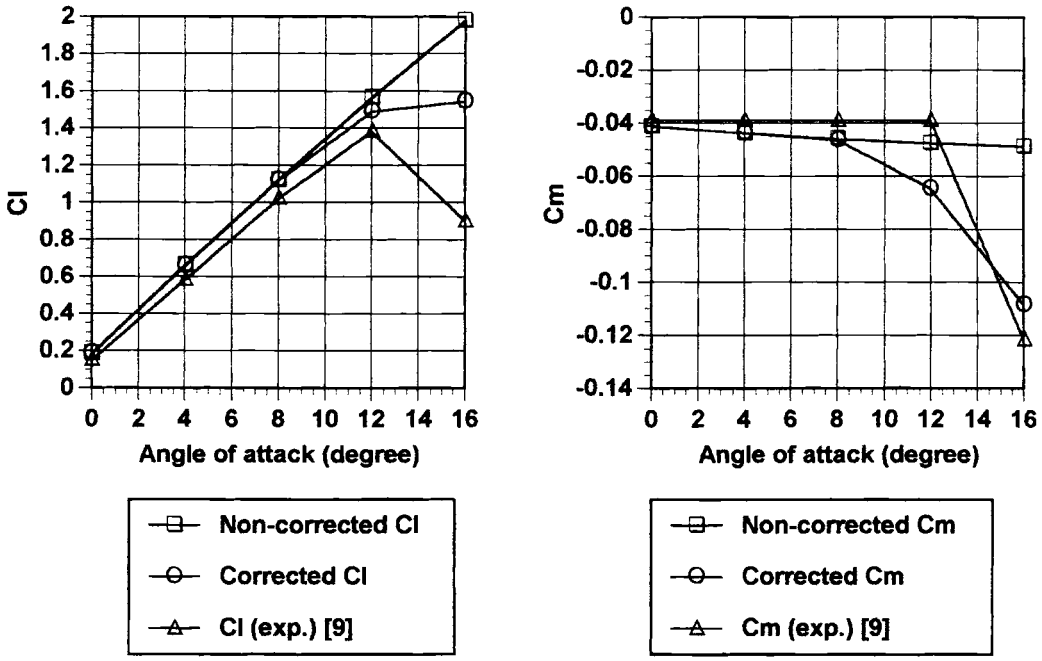

Figure 4.9. Corrected Cl, Cm on NACA63A210, Re=6,000,000

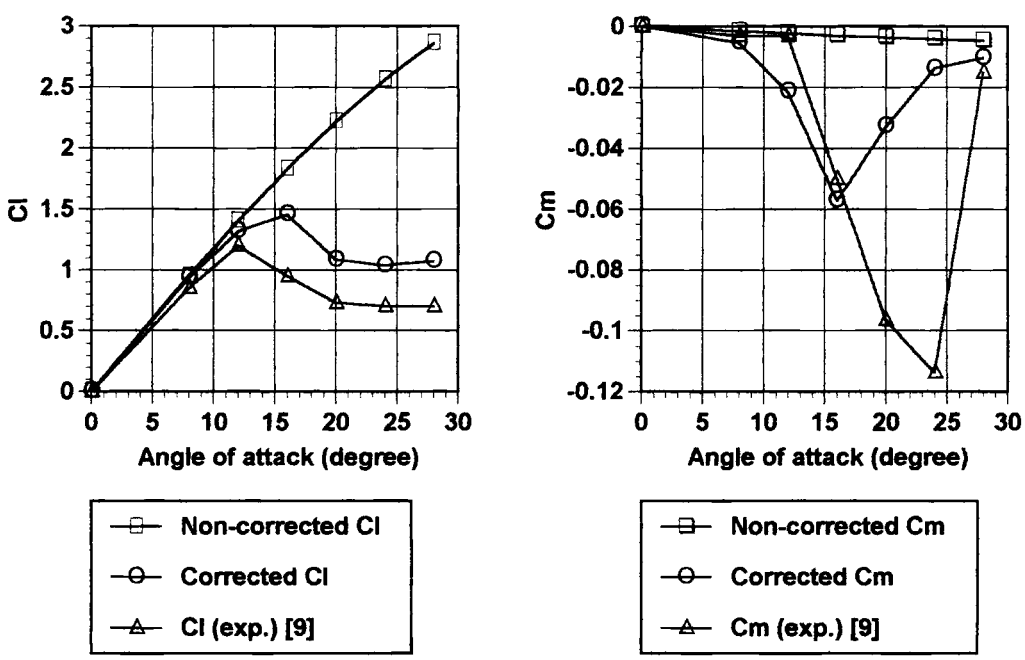

Figure 4.10. Corrected Cl, Cm on NACA0012, Re=1,800,000

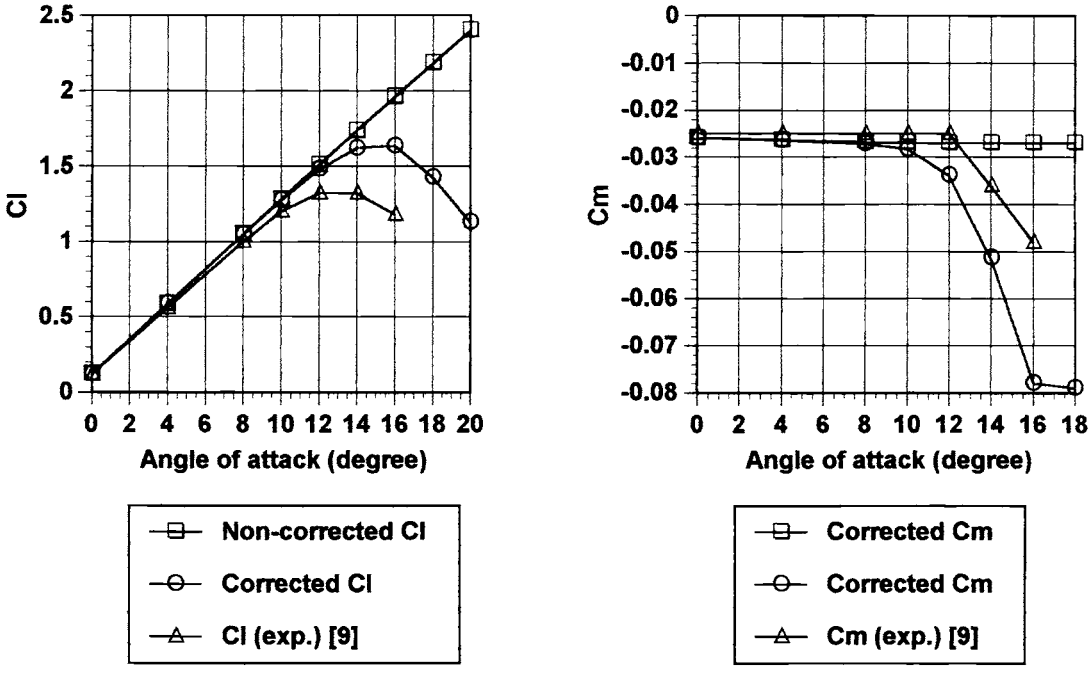

Figure 4.11. Corrected Cl, Cm on NACA1408, Re=9,000,000

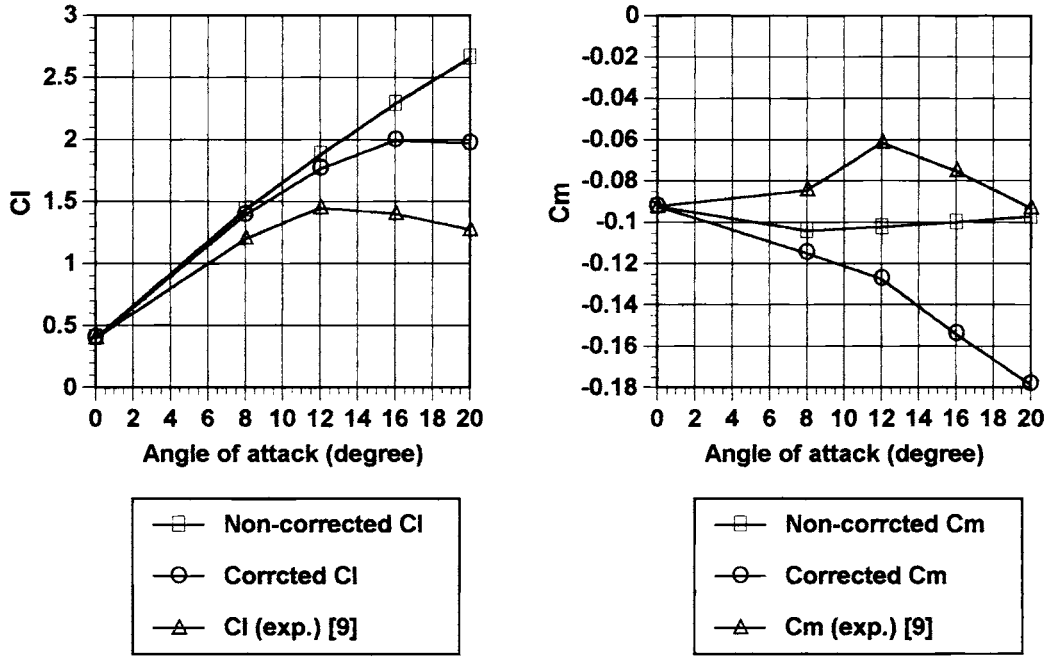

Figure 4.12. Corrected Cl, Cm on NACA4412, Re=3,000,000

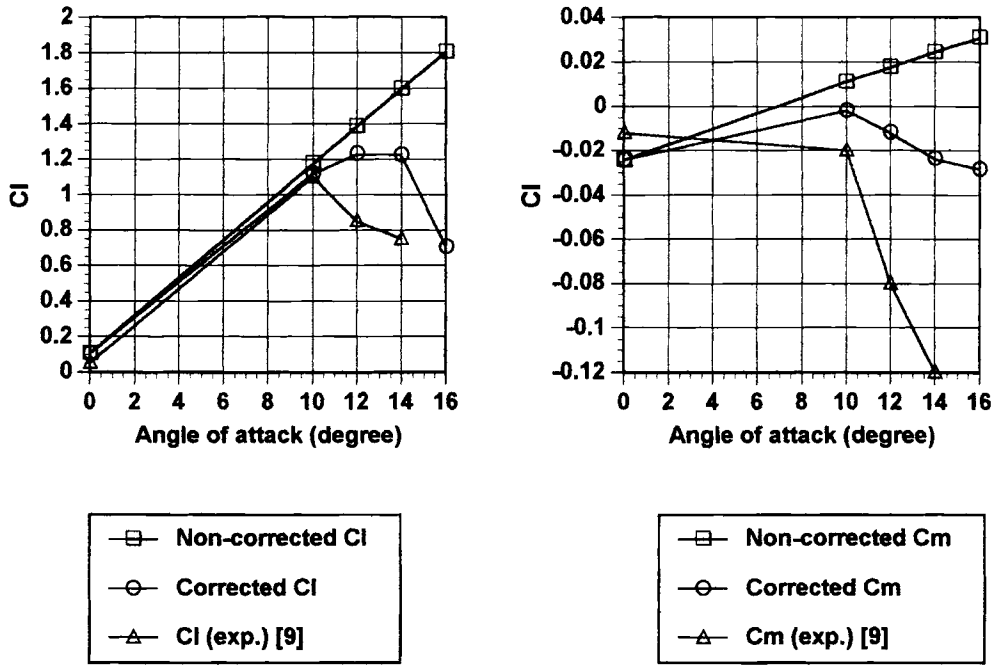

Figure 4.13. Corrected Cl, Cm on NACA64-108, Re=9,000,000

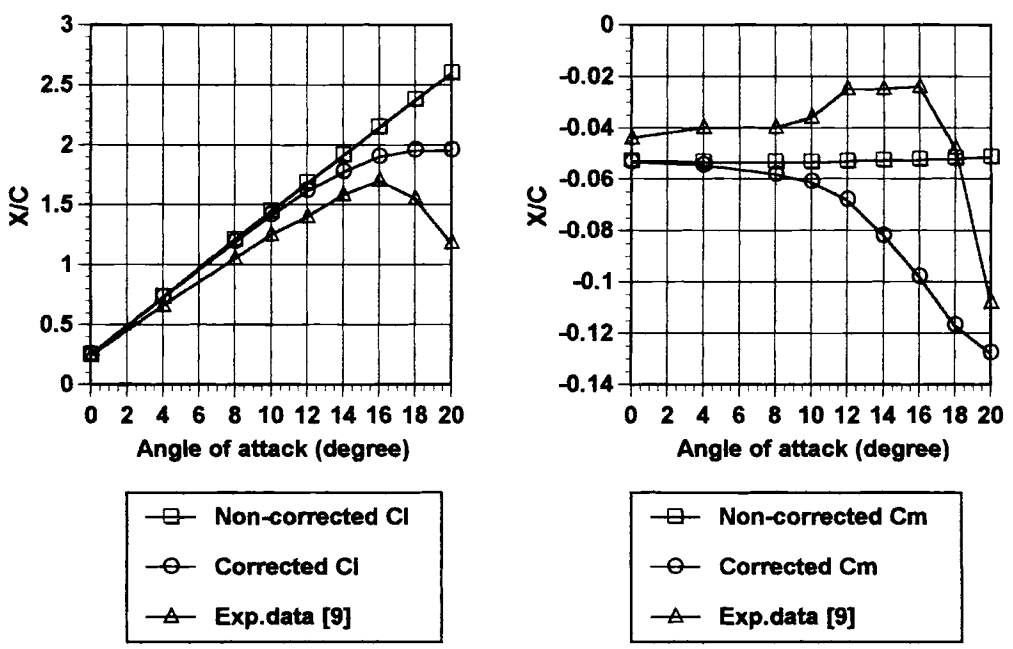

Figure 4.14. Corrected Cl, Cm on NACA2412, Re=5,700,000

Notice that in every cases the calculated Cl, Cm follow the characteristics of Cl, Cm experimental data surprisingly very well. Although the resultant aerodynamic characteristics by potential flow solutions cannot be relied on quantitatively, the potential flow solutions with integral-type separation prediction method can be used as a tool to estimate the airfoil's effectiveness qualitatively.

4.5 Sensitivity survey for the use of Integral method.

Integral method code starts running and calculating boundary layer solutions from the leading edge stagnation point using Thwaites's method. Assuming that the Reynolds number is so high that laminar separation is unlikely to occur, eventually the transition criterion is met and the transition to the turbulent boundary layer is assumed to exist. To shift to Head's method, the starting value of H for the turbulent boundary layer is needed. Moran [12] indicated that the initial value of H for the turbulent boundary layer is likely to be in the range 1.3 to 1.4. However, in the case of potential flow solution, H=1.5 seems to be appropriate for the code to predict the reasonable points of separation compared to experimental data.

The range of the starting value of H , with which the reasonable separation point can be calculated is studied. The results are seen in Figure 4.15.

With NACA0012 airfoil, the appropriate value of H lies between 1.4 to 1.9, which is a relatively wide range. On the other hand, in the case of NACA63$_2$-415, the value of H should be in the narrow range 1.5 to 1.6. In addition H=1.4-1.6 is required for NACA4412.

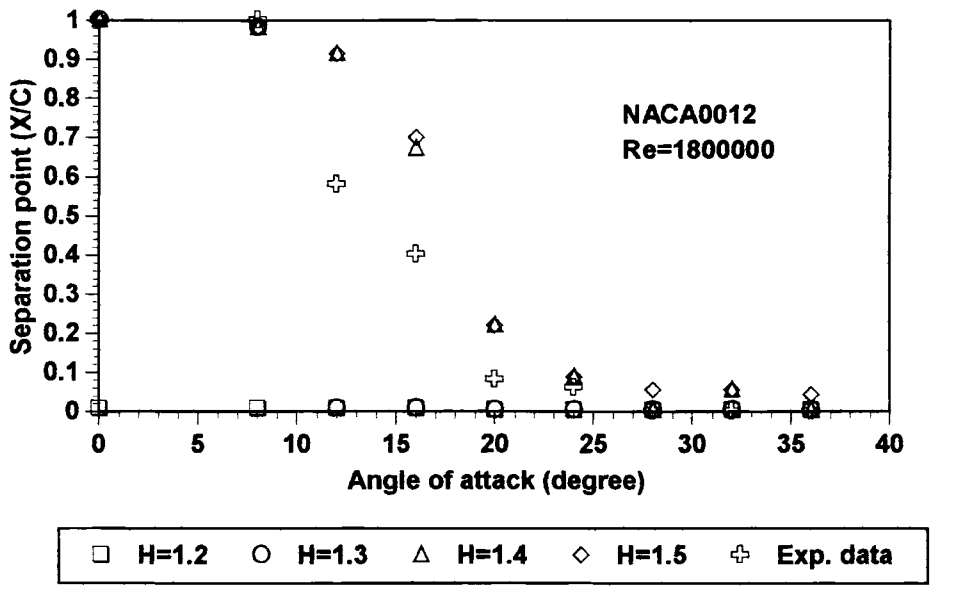

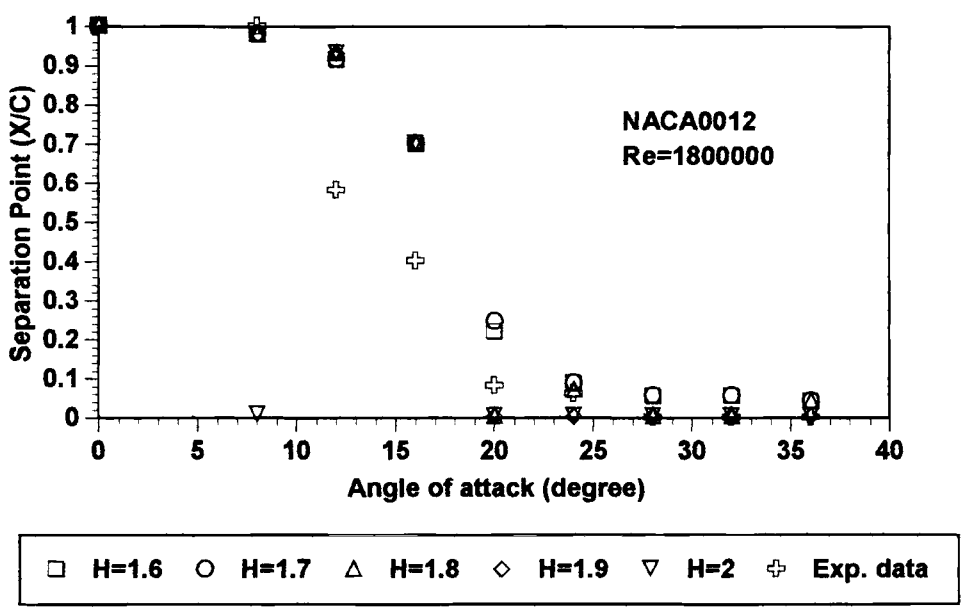

Figure 4.15. The predicted separation point by Integral method with the varied starting value of H for a turbulent boundary layer. (Experimental data(Exp.data) from [20])

Everything considered, in most cases, the starting value of H of 1.5 is appropriate for the turbulent boundary layer calculation.

Moran suggested in his book[12] that the starting value of H can be guessed, and this is not so rough as it may sound. The starting value of H for a turbulent boundary layer usually lies in a rather narrow range and it is seldom out of the range 1.3 to 1.4 [12].

According to the current study, this suggested range of H turns into H=1.5. Furthermore, the computational results indicates that the choice of the starting value of H largely affects the outcome. As seen in Figure 4.15 and other data collected, the inappropriate choice of the starting value of H causes the program to predict 'too' early separation.

4.6 Transition criteria

Other than the initial starting value of H discussed in the preceding section, the validity of transition criteria is needed to be investigated as well. In this survey, two transition criteria were prepared and applied to airfoils. They are Michel criterion and the point of maximum velocity criterion.

As seen in Figure 4.16, when applied to experimental pressure distribution, both criteria work very well. Whichever criterion is applied, the resultant separation points match the experimental data very well regardless of α. Moreover, the usage of each

criterion doesn't make any significant difference, the results by one criterion is almost exactly the same as those by the other. However, when applied to potential flow solutions, the choice of the criterion does make a difference as seen in Figure 4.17-18.

From the results in both Figure 4.17-18, it is concluded that Michel criterion, if applied to potential flow solutions, comes to predict unreasonably 'too' early separation compared to experimental data while the maximum velocity criterion is still well able to follow the experimental data qualitatively. Consequently, it can be said that the choice of Michel criterion should be considered inappropriate when potential flow solutions are dealt with.

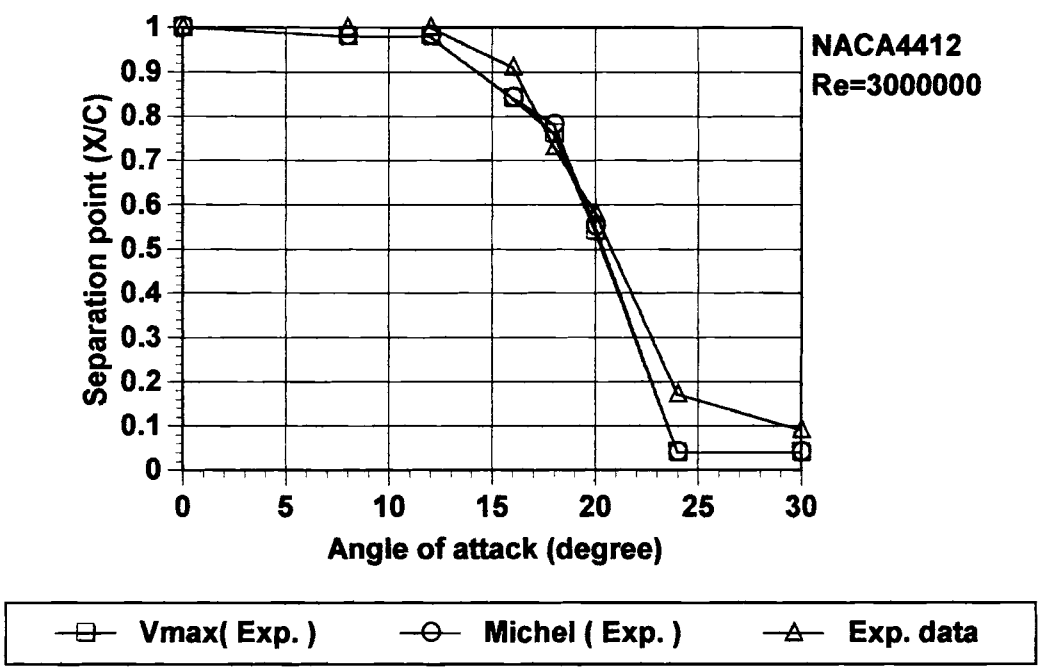

Figure 4.16 The predicted separation points by Integral method with two different transition criteria. Calculation is based on the pressure distribution from Experimental data (Exp.) from [19]. 'Exp.data' from [19]

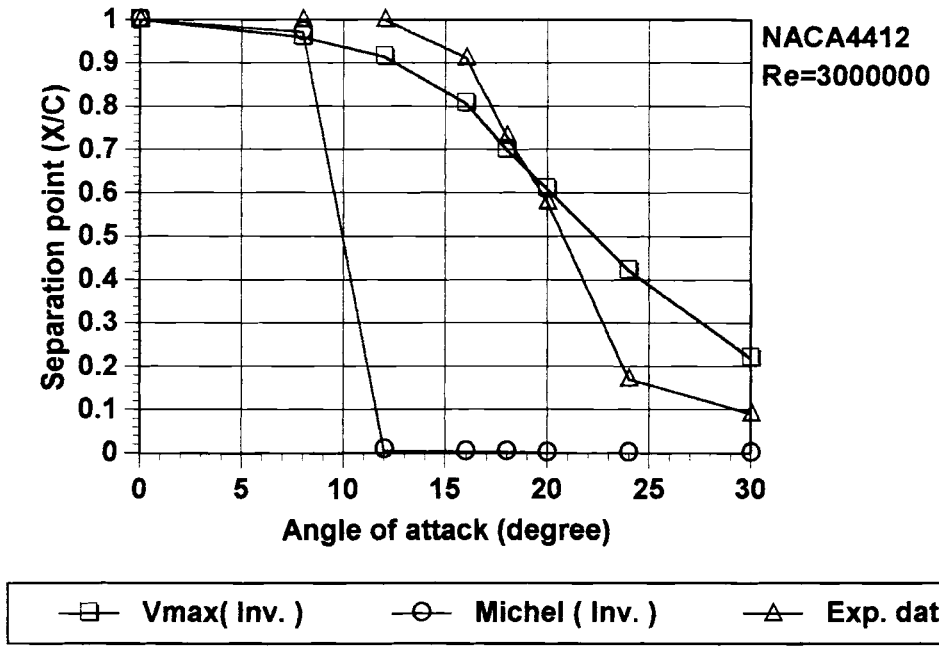

Figure 4.17. The predicted separation points by Integral method with two different transition criteria. Calculation is based on the pressure distribution from potential flow theory (Inv.) 'Exp.data' from [19] NACA4412, Re=3,000,000

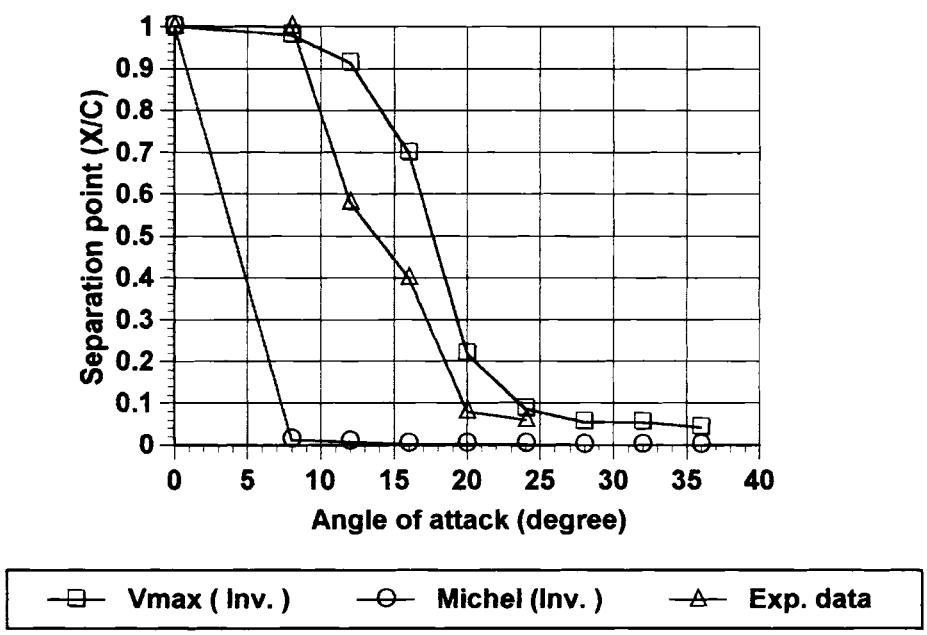

Figure 4.18. The predicted separation points by Integral method with two different transition criteria. Calculation is based on the pressure distribution from potential flow theory (Inv.) Exp.data from [19] NACA0012, Re=1,800,000

4.7 Validity of the maximum velocity criterion with potential flow solutions.

Validity of the maximum velocity criterion of transition point has been confirmed in the preceding section. the sensitivity of this criterion to the slight change of the point of transition point around the point of the maximum velocity has also been examined. the results are shown in Figure 4.19-21. In every case of an airfoil studied here regardless of α, there is always a certain region where the transition point to the turbulent boundary layer should locate. If the transition point is put in front of this region closer to the leading edge, Integral method program tends to predict the unreasonably 'too' early turbulent separation. On the other hand, if transition point is fixed after this region closer to the trailing edge, the code tends to indicate, again, 'too' early ,but, laminar separation. This phenomenon can be seen in Figure 4.18-20.

For example, in Figure 4.19 at the angle of attack of 8°, the distance of the transition point from the forward stagnation point should be 0.025 to 0.045, and if not, the unreasonable location of separation would be predicted. The same thing can be said in the case of α=16°.

In the case of α=24°, however, even if transition point is located within the range where transition point should be for reasonable outcome, depending on where exactly in this range transition point is put, the resulting separation point will vary. This characteristics can be observed in every airfoil case studied, Figure 4.19-21.

As the angle of attack is getting larger, the slight change of the location of transition point comes to result in the larger change of the position of the point of

separation. More importantly, this tendency is especially pronounced about the point of minimum pressure, that is , the high pressure gradient region. Therefore, when an airfoil is investigated with high α, the determination of transition point by the maximum velocity point option could be inappropriate while it is not totally invalid. Consequently, the location of transition should be considered with care.

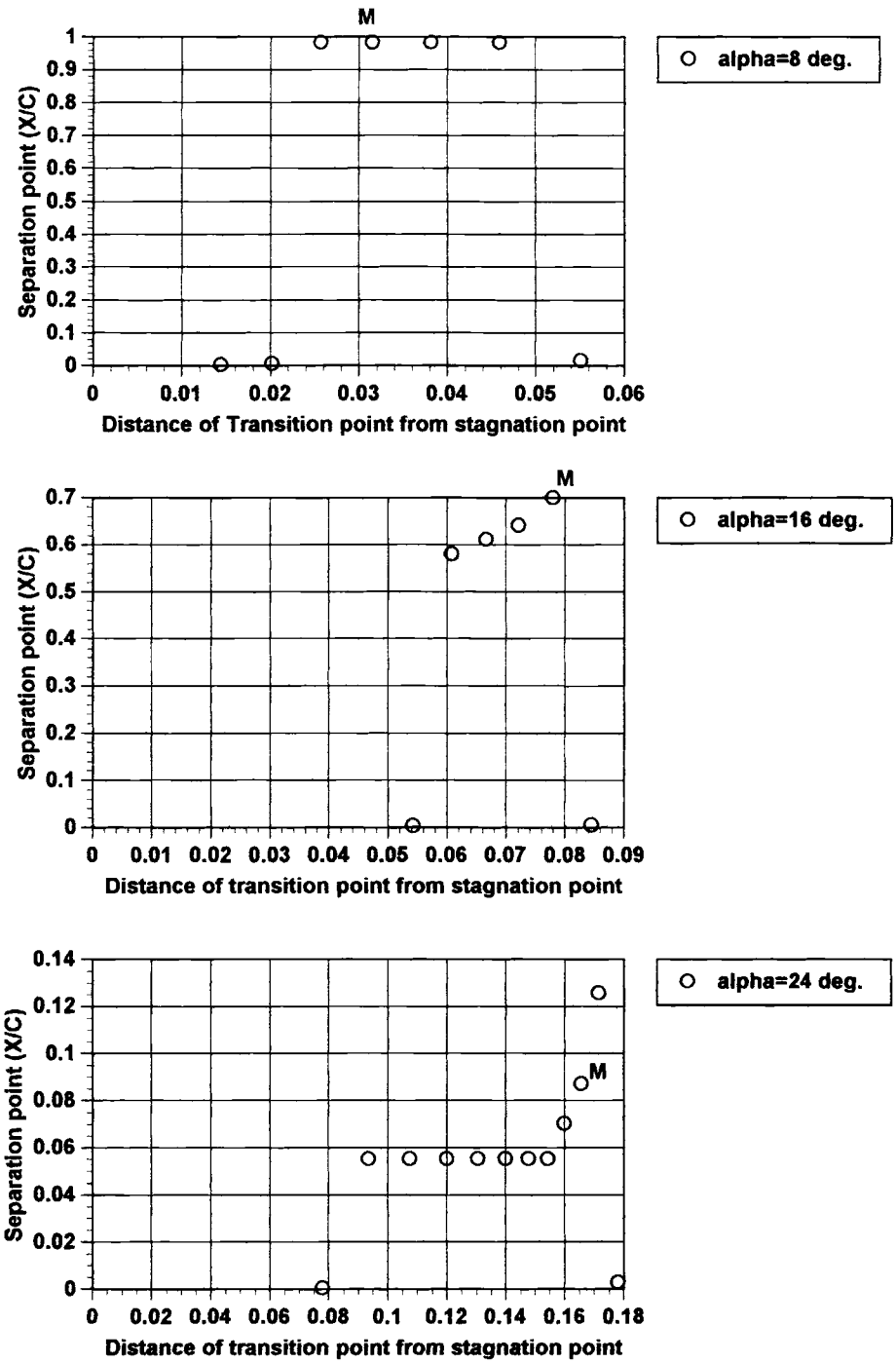

Figure 4.19. The change of the location of separation point with the location of transition point. "M" denotes the point of the maximum velocity. NACA0012,Re=1,800,000

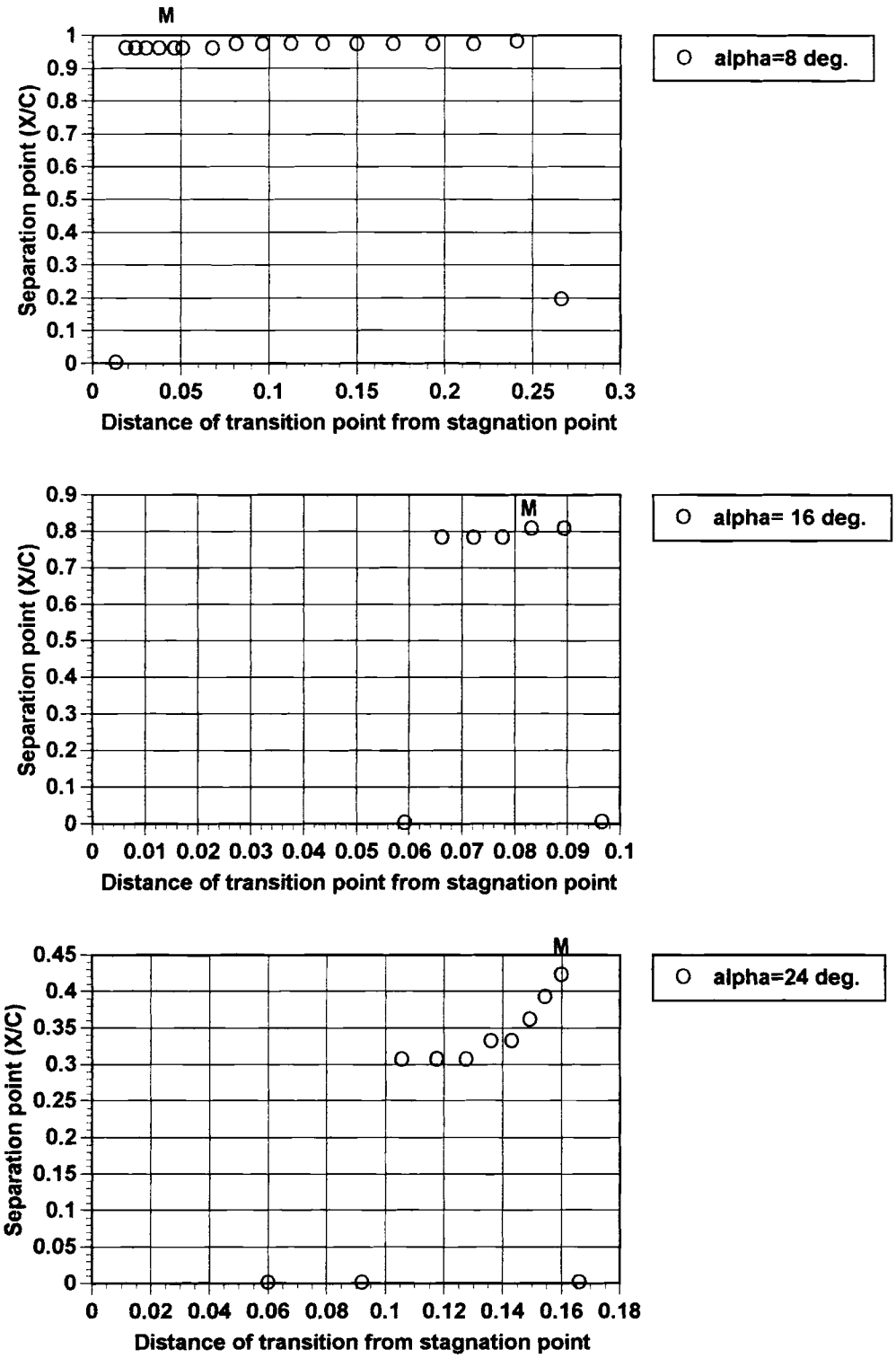

Figure 4.20. The change of the location of separation point with the location of transition point. "M" denotes the point of the maximum velocity. NACA4412,Re=3,000,000

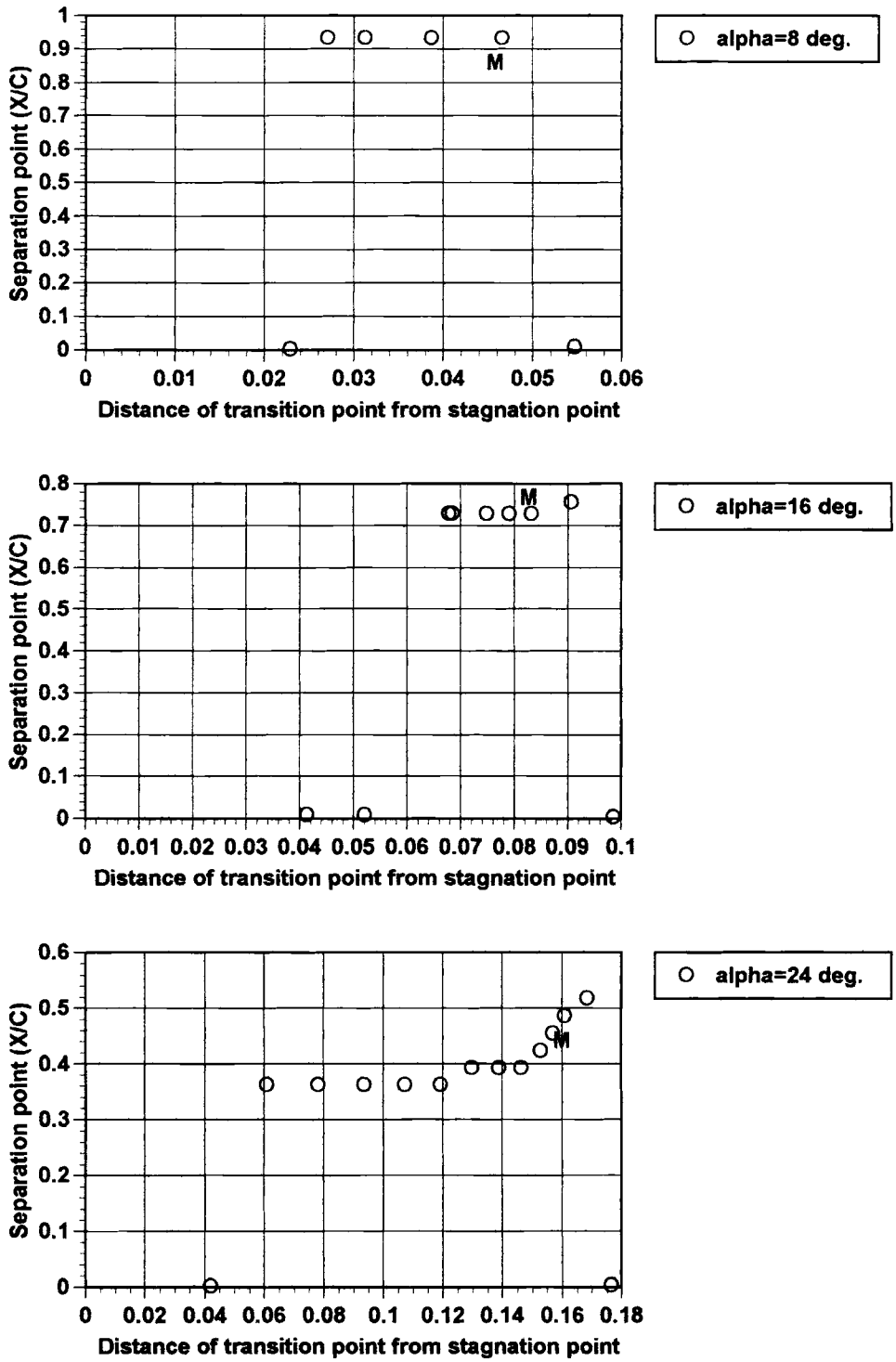

Figure 4.21. The change of the location of separation point with the location of transition point. "M" denotes the point of the maximum velocity. NACA63$_2$415 Re=6,000,000

4.8 The code validity for low Reynolds number

The code validity when applied with low Re has been examined and results are seen in Figure 4.22. This is very necessary to be done as a part of the current survey, because the maximum velocity point option was used to obtain computational data for the current study. As mentioned before in section 3.1.2, the determination of transition location based on the point of maximum velocity should be reasonable in the range of $Re=10^6 - 10^7$, and then all computational data obtained here were obtained in this range of Re.

If low Re is assumed, however, the validity of the maximum velocity option may become questionable. And then, the laminar boundary layer separation, which is not assumed to occur in the code, becomes more likely to occur. In this connection, the region where the code becomes invalid must be investigated.

The data for a single airfoil with wide range of Re were found rare so that the investigation was carried out with a circular cylinder case, because there are a lot of data available with broad range of Re. A circular cylinder case can be considered as a symmetric airfoil with large thickness ratio.

In Figure 4.22, notice that calculation with Michel criterion always predicts the laminar boundary layer separation around $\theta = 100°$. Michel criterion has been found to be invalid when applied to pressure distribution obtained by potential flow theory. Further, Michel criterion is developed for an airfoil-type pressure distribution where the point of minimum pressure usually locates relatively closer to the leading edge rather

than the half-chord position like cylinder case [12]. Then the results based on Michel criterion are of little importance.

The results with the maximum velocity option should be should be paid attention to. Where Re is below 1.5×10^5 there is a significant difference between computation results and experimental data. This is because the laminar boundary layer separation is observed in this region and experimental data surely indicates this happening. The laminar boundary separation is, however, not assumed to occur in the code as long as the maximum velocity-based transition point option is used.

When the laminar boundary layer separation is expected with low Re, the point of instability, after which transition is likely to occur, is located after the maximum velocity point, where in the code transition is assumed to initiate. This is true as long as $Re<1.5 \times 10^5$ in Figure 4.22. In other words, if applied to any case with $Re<1.5 \times 10^5$, the code will indicate the location of the turbulent layer separation, although the laminar boundary layer separation is supposed to be observed in this range of Re. So, in the calculation, a boundary layer is assumed to turn into turbulent at the point of maximum velocity, even though in a 'real' boundary layer transition never occurs due to the laminar boundary layer separation except the case of reattachment.

Hence, if one wants to run the code for low Re, $Re<1.5 \times 10^5$ for a circular cylinder case, one must be aware of possible invalidity of the results to be calculated.

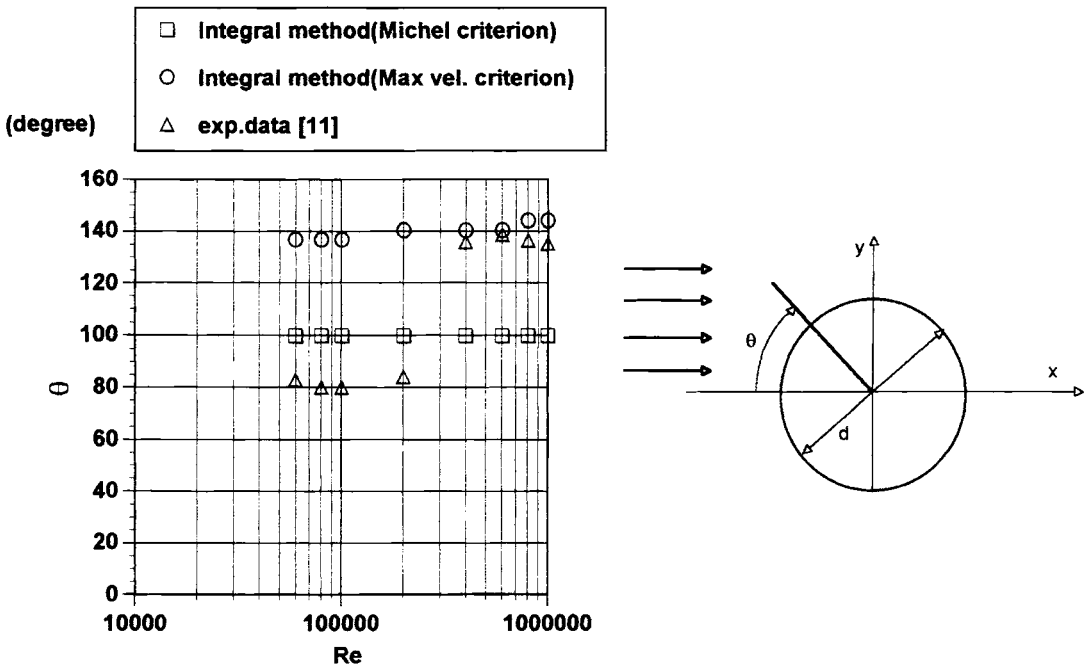

Figure 4.22 Location of separation points on a circular cylinder as a function of Reynolds number

CHAPTER V

CONCLUSIONS AND RECOMMENDATIONS

4.1 CONCLUSIONS

The goal of the current study was to investigate the accuracy of the prediction methods for predicting the turbulent boundary layer separation point with potential flow solutions. The chord-wise pressure distribution obtained by potential flow theory was applied to selected prediction methods. The two simple method not requiring detailed boundary layer calculation are, unfortunately, confirmed to be invalid when used with potential flow solutions. On the other hand, though its complexity is not easy to deal with, Integral-type methods canceled out the effect of the unrealistically sharp pressure spike near the leading edge and qualitatively captured the characteristics of flow separation of all the airfoils investigated here.

The computational results have also led to the conclusion that if potential flow solutions are used, the point of the maximum velocity can be used as the transition point to the turbulent boundary layer, while Michel transition criterion should be avoided. Then, it is found that by Integral-type method with the transition point based on the

maximum velocity point, it is possible qualitatively to capture the separation characteristics of an airfoil.

Furthermore, the aerodynamic characteristics, Cl, Cm, have been well corrected by the effect of separation predicted by Integral-type method so that the resultant aerodynamic characteristics would follow the experimental data surprisingly well. This also indicates that the efficiency of an airfoil can be qualitatively estimated without the wind tunnel-type large scale facility.

There are, some limitations to the use of potential flow solutions. The invalidity of Michel criterion has been studied, and the propriety of the determination of the separation point by the maximum velocity transition criterion were confirmed.

However, with the flow of low Reynolds number, Re $< 10^6$, the laminar separation is likely to occur after the point of the maximum velocity. So, the code can predict the turbulent boundary layer separation where the laminar boundary separation is supposed to occur. Then, if applied to such a flow, the Integral method code should be handled more carefully. In that case, it is necessary to examine the most likely point of transition by 'trial-and-error' and comparison to the experimental data available. In spite of this low Reynolds number flow handling difficulty, in most cases the airfoil is studied with higher Reynolds number ($10^6 - 10^7$) so that the problem mentioned above hardly matters.

4.2 Recommendations

An integral-type computational prediction method can be used as a tool by which the boundary layer separation may qualitatively be analyzed with potential flow solutions in an efficient manner. The possibility for the direction of further developments and enhancements of the code are endless.

Especially, further improvement of more dependable and flexible transition criterion for broader range of Reynolds number shall be considered. Also, separation bubble, or boundary layer reattachment and bubble warning can be implemented, which may strengthen the applicability of the code.

REFERENCES

1. Arnold M. Kuethe and Chuen-Yen Chow "Foundations of Aerodynamics: Bases of Aerodynamic of Aerodynamic Design" John & Sons, Inc., 1986

2. B. S. Stratford. "The Prediction of separation of the turbulent boundary layer" Journal of Fluid Mechanics, Vol. 5, 1959

3. Chris C. Critzos and Harry H. Heyson. "Aerodynamic characteristics of NACA0012 Airfoil section at Attack from 0° to 180° " NACA TN 3361, 1956

4. E. Achenbach. "Distribution of Local Pressure and Skin Friction Around a Circular Cylinder in Cross-Flow up to $Re = 5 \times 10^6$" Journal of Fluid Mechanics, Vol. 34, Part 4, 1968

5. Farbio R, Goldschmied. "An Approach to Turbulent Incompressible Separation under Adverse Pressure Gradients" Journal of Aircraft, Vol. 2, No.1 1964

6. Frank M. White. "Viscous Fluid Flow" McGraw-Hill, Inc., 1991

7. Friedrich W. Riegels "Airfoil Sections : Results from wind-tunnel investigations theoretical foundations" London, Butterworth & Co. Ltd., 1961

8. Hermann Schlichting "Boundary Layer Theory" McGrow-Hill Book Company, 1987

9. Ira H. Abbot and Albert E. Von Doenhoff "Theory of Wing Sections : Including a Summary of Airfoil Data" New York, Dover Publications, Inc. 1959

10. Joseph Katz and Allen Plotkin. "Low-speed Aerodynamics : From Wing Theory to Panel Methods." McGraw-Hill, Inc., 1991

11. John J. Bertin and Michael L. Smith. "Aerodynamics For Engineering" New Jersey Prentice-Hall, Inc., 1989

12. Jack Moran. "An Introduction to Theoretical and Computational Aerodynamics" John Wiley & Sons, Inc., 1984

13. Martin Simons. "Model Aircraft Aerodynamics" Argus books, 1994

14. N. Curle. "The Laminar Boundary Layer Equations" Oxford at the Clarendon Press, 1962

15. Rechard Eppler "Airfoil Design Data" Springer-Verlag, 1990

16. Robert H. Liebeck. "A class of Airfoils Designed for High Lift in Incompressible Flow" Journal of Aircraft Vol. 10, No.10 1973

17. Robert H. Liebeck. " Optimization of Airfoils for Maximum Lift" Journal of Aircraft Vol. 7, No. 5 1970

18. T. Cebeci and A.M.O. Smith. "A Finite-Difference Method for Calculating Compressible Lminar and Turbulent Boundary Layers" Journal of Basic Engineering, Vol.92, No.3

19. T. Cebeci, G. J. Monsinskis and A.M.O. Smith. "Calculation of Separation Points in Compressible Turbulent Flows" Journal of Aircraft Vol.9 , No.9 1972

20. T.K. Perfito and A.S. Arena, Jr. "A 2-D Approach to Modelling Longitudinal Dynamics in Stall Flight" AIAA 94-0809, AIAA 32nd Aerospace Sciences Meeting & Exhibit, January, 1994

APPENDIXES

- Stratford's method code..... 'predictx.for'
- Goldschmied's method code ..... 'goldx.for'
- Integral method code
(Thwaites-Head's combined method) ..... 'intgrl4.for'
- Panel method code (Inviscid flow solver) ... 'smhess.for'
- Code validation

```
c**********************************************************************
c
c    program predictx.f
c
c    This program is to predict a separation point by Stratford's method with a given Cp
c    distribution.
c
c**********************************************************************

      integer k,i,numcpm,numtrans,datanumber,stagpoint,datamax
      real psx(200),psy(200),pcp(200),pu(200),x(200)
      real pi,sx(200),sy(200),cp(200),ds(200),d(200)
      real bcp(200),gradbcp(200)
      real strat(200),dueui5(200),ueui5
      real cpm,nu,bre,re,c,uinf,u(200)
      real gradcp(200),grad2cp(200)

      datanumber=100
      write(*,*)'Input Re#'
      read(*,*)re
c     re=3000000
      nu=14.4e-6
      c=1
      pi=4.*atan(1.)
      open(5,file='cps.dat')
      open(10,file='strat.dat')
      open(15,file='checkgeo.dat')

      uinf=re*nu/c

c****** Read input file (Cp distribution) ******************

      stagpoint=0
      k=0
      do 8 i=1,datanumber
      read(5,*)psx(i),psy(i),pcp(i),pu(i)
      if ((pu(i).ge.0).and.(k.eq.0)) then
        stagpoint=i
        k=1
      endif
8     continue

c****** Reorder data starting from Stagnation Point *******

      datamax=datanumber-stagpoint+1

      do 12 i=1,datamax
        sx(i)=psx(stagpoint-1+i)
        sy(i)=psy(stagpoint-1+i)
        cp(i)=pcp(stagpoint-1+i)
        u(i)=pu(stagpoint-1+i)
        write(15,*)sx(i),sy(i),cp(i),u(i)
12    continue
```

```
c****** Calculate ds,d from input data ********************

    d(1)=0
    do 80 i=2,datamax
      ds(i)=sqrt((sx(i)-sx(i-1))**2+(sy(i)-sy(i-1))**2)
      d(i)=d(i-1)+ds(i)
80   continue



c******* Find a point of Cpm where Ue is maximum **********

    cpm=1
    numcpm=0
    do 10 i=1,datamax
      if(cp(i).lt.cpm) then
      cpm=cp(i)
      numcpm=i
      endif
10   continue

    write(*,*) cpm,numcpm
    numtrans=numcpm

c****** Calculate _Cp ************************************

     do 15 i=1,datamax
       bcp(i)=(cp(i)-cpm)/(1-cpm)
15     continue

c****** Calculate dCp/dx *********************************

    do 22 i=1,datamax
      if(i.eq.1) then
        gradcp(1)=(cp(2)-cp(1))/ds(2)
      elseif(i.eq.datamax) then
        gradcp(datamax)=(cp(datamax)-cp(datamax-1))/ds(datamax)
      else
        gradcp(i)=(cp(i+1)-cp(i-1))/(ds(i)+ds(i+1))
      endif
22   continue

c****** Calculate d_Cp/dx *********************************

    do 20 i=1,datamax
      if(i.eq.1) then
        gradbcp(1)=(bcp(2)-bcp(1))/ds(2)
      elseif(i.eq.datamax) then
        gradbcp(datamax)=(bcp(datamax)-bcp(datamax-1))/ds(datamax)
      else
```

```
        gradbcp(i)=(bcp(i+1)-bcp(i-1))/(ds(i)+ds(i+1))
      endif
20    continue

c****** Calculate d2Cp/dx *********************************

      do 24 i=1,datamax
        if(i.eq.1) then
          grad2cp(1)=(gradcp(2)-gradcp(1))/ds(2)
        elseif(i.eq.datamax) then
          grad2cp(datamax)=(gradcp(datamax)-gradcp(datamax-1))
     +                    /ds(datamax)
        else
          grad2cp(i)=(gradcp(i+1)-gradcp(i-1))/(ds(i)+ds(i+1))
        endif
24    continue


c****** Calculate Xm ***************************************

      do 25 i=1,numtrans
        dueui5(i)=((1-cp(i))/(1-cp(numtrans)))**2.5
c       dueui5(i)=(u(i)/u(numtrans))**5
25    continue

      ueui5=0
      do 30 i=2,numtrans
        ueui5=ueui5+(dueui5(i)+dueui5(i-1))/2*ds(i)
30    continue

      xm=38.2*(nu/(u(numtrans)*uinf))**.375*ueui5**.625

      write(*,*)xm

c****** Calculate X at points after the point of Umax ****

      do 35 i=numcpm,datamax
        x(i)=d(i)-d(numcpm)+xm
35    continue

      bre=u(numcpm)*uinf*xm*c/nu

c****** Apply Stratford's method to those points **********

      do 40 i=numcpm+2,datamax
        strat(i)=bcp(i)*sqrt(x(i)*gradbcp(i))/((1e-6*bre)**(.1))
        write(10,*) sx(i),x(i),gradbcp(i),strat(i)
40    continue
      close(5)
      close(10)
      close(15)
      stop
      end
```

```
c**********************************************************************
c
c    program GOLDX.for
c
c    This program is to predict a separation point by Goldschmied's method with a given Cp
c    distribution.
c
c**********************************************************************

      integer k,i,numcpm,numtrans,datanumber,stagpoint,datamax
      real psx(200),psy(200),pcp(200),pu(200),x(200)
      real pi,sx(200),sy(200),cp(200),ds(200),d(200)
      real bcp(200),gradbcp(200)
      real strat(200),dueui5(200),ueui5
      real cpm,nu,bre,re,c,uinf,u(200)
      real gradcp(200),grad2cp(200),cfm

      datanumber=100
      write(*,*)'Input Re#'
      read(*,*)re
c     re=3000000
      nu=14.4e-6
      c=1
      pi=4.*atan(1.)
      open(5,file='cps.dat')
      open(10,file='gold.dat')
      open(15,file='checkgeo.dat')

      uinf=re*nu/c

c****** Read input file (Cp distribution) ******************

      stagpoint=0
      k=0
      do 8 i=1,datanumber
      read(5,*)psx(i),psy(i),pcp(i),pu(i)
      if ((pu(i).ge.0).and.(k.eq.0)) then
        stagpoint=i
        k=1
      endif
8     continue

c****** Reorder data starting from Stagnation Point *******

      datamax=datanumber-stagpoint+1

      do 12 i=1,datamax
        sx(i)=psx(stagpoint-1+i)
        sy(i)=psy(stagpoint-1+i)
        cp(i)=pcp(stagpoint-1+i)
        u(i)=pu(stagpoint-1+i)
        write(15,*)sx(i),sy(i),cp(i),u(i)
12    continue
```

```
c****** Calculate ds,d from input data ********************

    d(1)=0
    do 80 i=2,datamax
      ds(i)=sqrt((sx(i)-sx(i-1))**2+(sy(i)-sy(i-1))**2)
      d(i)=d(i-1)+ds(i)
80   continue


c******* Find a point of Cpm where Ue is maximum **********

    cpm=1
    numcpm=0
    do 10 i=1,datamax
      if(cp(i).lt.cpm) then
      cpm=cp(i)
      numcpm=i
      endif
10   continue

    write(*,*) cpm,numcpm
    numtrans=numcpm

c****** Calculate _Cp ************************************

     do 15 i=1,datamax
       bcp(i)=(cp(i)-cpm)/(1-cpm)
15    continue

c****** Calculate dCp/dx *********************************

    do 22 i=1,datamax
      if(i.eq.1) then
        gradcp(1)=(cp(2)-cp(1))/ds(2)
      elseif(i.eq.datamax) then
        gradcp(datamax)=(cp(datamax)-cp(datamax-1))/ds(datamax)
      else
        gradcp(i)=(cp(i+1)-cp(i-1))/(ds(i)+ds(i+1))
      endif
22   continue

c****** Calculate d_Cp/dx *********************************

    do 20 i=1,datamax
      if(i.eq.1) then
        gradbcp(1)=(bcp(2)-bcp(1))/ds(2)
      elseif(i.eq.datamax) then
        gradbcp(datamax)=(bcp(datamax)-bcp(datamax-1))/ds(datamax)
      else
        gradbcp(i)=(bcp(i+1)-bcp(i-1))/(ds(i)+ds(i+1))
```

```
      endif
20    continue

c****** Calculate d2Cp/dx *********************************

      do 24 i=1,datamax
        if(i.eq.1) then
          grad2cp(1)=(gradcp(2)-gradcp(1))/ds(2)
        elseif(i.eq.datamax) then
          grad2cp(datamax)=(gradcp(datamax)-gradcp(datamax-1))
     +                    /ds(datamax)
        else
          grad2cp(i)=(gradcp(i+1)-gradcp(i-1))/(ds(i)+ds(i+1))
        endif
24    continue


c****** Calculate Xm ***************************************

      do 25 i=1,numtrans
        dueui5(i)=((1-cp(i))/(1-cp(numtrans)))**2.5
c       dueui5(i)=(u(i)/u(numtrans))**5
25    continue

      ueui5=0
      do 30 i=2,numtrans
        ueui5=ueui5+(dueui5(i)+dueui5(i-1))/2*ds(i)
30    continue

      xm=38.2*(nu/(u(numtrans)*uinf))**.375*ueui5**.625

      write(*,*)xm
      write(*,*)'Rex=',re*xm
      write(*,*)'200Cf=',200*0.664/sqrt(re*xm)

c****** Calculate X at points after the point of Umax ****

      do 35 i=numcpm,datamax
        x(i)=d(i)-d(numcpm)+xm
35    continue

      bre=u(numcpm)*uinf*xm*c/nu
      cfm=.73/sqrt(bre)
c****** Apply Stratford's method to those points **********

      do 40 i=numcpm+2,datamax
        strat(i)=bcp(i)*sqrt(x(i)*gradbcp(i))/((1e-6*bre)**(.1))
        write(10,*) sx(i),x(i),bcp(i),200*cfm
40    continue
      close(5)
      close(10)
      close(15)
      stop
      end
```

```
c*************************************************************************
c
c       PROGRAM INTGRL4.FOR
c
c       INTEGRAL METHOD FOR CALCULATION OF BOUNDARY LAYER
c       GROWTH ON AN AIRFOIL, STARTING AT A STAGNATION POINT
c
c       THWAITES'S METHOD USED FOR LAMINAR-LAYER FLOW
c       MICHEL AND THE MAX. VEL. CRITERIA USED TO FIX TRANSITION
c       HEAD'S METHOD USED FOR TURBULENT-FLOW REGION
c
c*************************************************************************

        COMMON /NUM/ PI,NX
        DIMENSION  YY(200)
        COMMON  XX(200),VGRAD(200),THETA(200)
        COMMON /INP1/ PSX(200),PSY(200),PCP(200),PVE(200)
        COMMON /INP2/ X(200),Y(200),CP(200),VE(200)
        COMMON /REY/ RE
        COMMON /BOD/ TAU
        REAL  LAMBDA, L
        INTEGER IANS,DATANUMBER,VELMAX,NX,CHOSEN

        PI = 3.1415926535
        DATANUMBER = 100

        OPEN( 5,FILE='cps.dat')
        OPEN(10,FILE='datacheck.dat')

c
c       READ INPUT FILE
c

        STAGPOINT = 1
        K = 0

        DO 8 I=1,DATANUMBER
         READ(5,*)PSX(I),PSY(I),PCP(I),PVE(I)
         IF((PVE(I) .GE. 0.0) .AND. (K .EQ. 0)) THEN
          STAGPOINT = I
          K = 1
         ENDIF
8       CONTINUE

        CLOSE (UNIT=5)

c
c       RE-ORDER DATA STARTING AT STAGNATION POINT
c

        NX = DATANUMBER - STAGPOINT +1

        DO 12 I=1,NX
         X(I) = PSX(STAGPOINT - 1 + I)
```

```
          Y(I) = PSY(STAGPOINT - 1 + I)
          CP(I) = PCP(STAGPOINT - 1 + I)
          VE(I) = PVE(STAGPOINT - 1 + I)
          WRITE(10,*)X(I),Y(I),CP(I),VE(I)
12        CONTINUE

          CLOSE(UNIT=10)
c
c         FIND THE POINT WHERE VE is MAXIMUM
c

          CPM = 1
          VELMAX = 1
          DO 10 I=1,NX
           IF(CP(I) .LT. CPM) THEN
            CPM = CP(I)
            VELMAX = I
           ENDIF
10        CONTINUE
          write(*,*) CPM,VELMAX

c
c         FIND DISTANCES BETWEEN NODES ALONG SURFACE
c

          XX(1) = 0.0
          DO 100 I=2,NX
           DX = X(I) - X(I-1)
           DY = Y(I) - Y(I-1)
100       XX(I) = XX(I-1) + SQRT(DX * DX + DY * DY)

c
c         FIND VELOCITY GRADIENT AT NODES
c

          V1 = VE(3)
          X1 = XX(3)
          V2 = VE(1)
          X2 = XX(1)
c         VE(NX+1) = VE(NX-2)
          XX(NX+1) = XX(NX-2)
          DO 110 I=1,NX
           V3 = V1
           X3 = X1
           V1 = V2
           X1 = X2
           V2 = VE(NX-2)
           IF(I .LT. NX)   V2 = VE(I+1)
            X2 = XX(I+1)
            FACT = (X3-X1)/(X2-X1)
            VGRAD(I) = ((V2 - V1)*FACT - (V3 - V1)/FACT)/(X3 - X2)
110       CONTINUE

c
```

```
c       SELECT TRANSITION CRITERION
c
        WRITE(*,*) 'DO YOU WANT TO FIX TRANSITION (1)'
        WRITE(*,*) 'OR USE MICHELS CRITERION (0)'
        WRITE(*,*) 'OR ELSE (2)'
        READ(*,*) IANS
        IF (IANS .EQ. 0)  GOTO 120
        IF (IANS .EQ. 1)  THEN
        XTRANS = X(VELMAX)
        GOTO 120
        ENDIF
c
c       IF FIXED TRANSITION POINT CHOSEN,
c       MAX VEL POINT IS TO BE TRANSITION POINT
c
        XTRANS = X(VELMAX)

c       WRITE(*,*) 'INPUT TRANSITION LOCATION'
c       READ(*,*) XTRANS

115     WRITE(*,*) 'INPUT DATA # (1 = STAGNATION POINT)'
        READ(*,*) CHOSEN

        XTRANS = XX(CHOSEN)
        WRITE(*,*) XX(CHOSEN)

c
c       INPUT REYNOLDSNUMBER BASED ON REFERRENCE V AND L
c
120     WRITE(*,*) 'INPUT Re'
        READ(*,*) RE
        WRITE(6,1000)

c
c       LAMINAR-FLOW REGION
c
        THETA(1) = SQRT(.075/RE/VGRAD(1))
        I = 1
200     LAMBDA = THETA(I)**2 * VGRAD(I)*RE
        IF(LAMBDA .LT. -.0842)  GOTO 400
        CALL THWATS(LAMBDA,H,L)
        CF = 2. * L/RE/THETA(I)
        IF(I .GT. 1)  CF = CF/VE(I)
        WRITE(6,1010) X(I),Y(I),VE(I),VGRAD(I),THETA(I),H,CF
        I = I + 1
        IF(I .GT. NX)    STOP
        DTH2VE6 = .225 * (VE(I)**5 + VE(I-1)**5) * (XX(I) - XX(I-1))/RE
        THETA(I) = SQRT(((THETA(I-1)**2) * (VE(I-1)**6) + DTH2VE6)
   +        /(VE(I)**6))
        IF(I .EQ. 2)    THETA(2) = THETA(1)
```

```
c
c       TEST FOR TRANSITION
c

        IF(IANS .EQ. 0)  GOTO 210

        IF(IANS .EQ. 1)  GOTO 215

        IF(XX(I) .LE. XTRANS)  GOTO 200
        GOTO 300

215     IF((X(I) .GT. XTRANS) .AND. (Y(I) .GT. 0.0)) GOTO 300
        GOTO 200

210     REX = RE * XX(I) * VE(I)
        RET = RE * THETA(I) * VE(I)
        RETMAX = 1.174 * (1. + 22400./REX) * REX**.46
        IF(RET .LT. RETMAX)   GOTO 200

c
c       TURBULENT-FLOW REGION
c

300     ITRANS = I
310     WRITE(*,*) 'INPUT H AT TRANSITION'
        READ(*,*) H
        IF(H .LT. 1.0)   STOP
        I = ITRANS
        YY(2) = H1OFH(H)
        YY(1) = THETA(I-1)
320     DX = XX(I)-XX(I-1)
        CALL RUNGE2(I-1,I,DX,YY,2)
        THETA(I) = YY(1)
        H = HOFH1(YY(2))
        RTHETA = RE * VE(I) * THETA(I)
        CF = CFTURB(RTHETA,H)
        WRITE(6,1020) X(I),Y(I),VE(I),VGRAD(I),THETA(I),H,CF
        IF(H .GT. 2.4)  GOTO 410
        I = I + 1
        IF(I .LE. NX)  GOTO 320
        STOP

400     WRITE(*,*) 'LAMINAR SEPARATION'
        STOP
410     WRITE(*,*) 'TURBULENT SEPARATION'
        GOTO 310

1000    FORMAT(///,9X,'X',8X,'Y',7X,'VE',6X,'VDOT',5X,'THETA',8X,'H',
     +    8X,'CF',/)
1010    FORMAT(' L',F10.5,F9.5,2F9.4,F11.7,F9.4,F10.6)
1020    FORMAT(' T',F10.5,F9.5,2F9.4,F11.7,F9.4,F10.6)
1030    FORMAT(A1)
```

```
      END
c=======================================================================
      SUBROUTINE THWATS(LAMBDA,H,L)
c
c     THWAITES'S CORRELATION FORMULAS
c
      REAL L,LAMBDA

      IF(LAMBDA .LT. 0.0)  GOTO 100
      L = .22 + LAMBDA * (1.57 - 1.8 * LAMBDA)
      H = 2.61 - LAMBDA * (3.75 - 5.24 * LAMBDA)
      GOTO 200
100   L = .22 + 1.402 * LAMBDA + .018 * LAMBDA/(.107 + LAMBDA)
      H = 2.088 + .0731 /(.14 + LAMBDA)
200   RETURN
      END
c=======================================================================
      FUNCTION H1OFH(H)
c
c     HEAD'S CORRELATION FORMULA FOR H1(H)
c
      IF(H .GT. 1.6)  GOTO 100
      H1OFH = 3.3 + .8234 * (H - 1.1)**(-1.287)
      RETURN
100   H1OFH = 3.3 + 1.5501 * (H - .6778)**(-3.064)
      RETURN
      END
c=======================================================================
      FUNCTION HOFH1(H1)
c
c     INVERSE OF H1(H)
c
      IF(H1 .LT. 3.3)  GOTO 110
      IF(H1 .LT. 5.3)  GOTO 100
      HOFH1 = 1.1 + .86 * (H1 - 3.3)**(-.777)
      RETURN
100   HOFH1 = .6778 + 1.1536 * (H1 - 3.3)**(-.326)
      RETURN
110   HOFH1 = 3.0
      RETURN
      END
c=======================================================================
```

```
      FUNCTION CFTURB(RTHETA,H)
c
c     LUDWIEG-TILLMAN SKIN FRICTION FORMULA
c

      CFTURB = .246 * (10. **(-.678 * H)) * (RTHETA)**(-.268)
      RETURN
      END

c=====================================================================

      SUBROUTINE DERIVS(I)
c
c     SET DERIVATIVES OY VECTOR Y
c

      COMMON /RNK/ YT(200),YP(200)
      COMMON       XX(200),VGRAD(200),THETA(200)
      COMMON /INP2/ X(200),Y(200),CP(200),VE(200)
      COMMON /REY/ RE

      H1 = YT(2)
      IF(H1 .LE. 3.)  RETURN
      H = HOFH1(H1)
      RTHETA = RE * VE(I) * YT(1)
      YP(1) = -(H + 2.) * YT(1) *VGRAD(I)/VE(I) + .5 * CFTURB(RTHETA,H)
      YP(2) = -H1 * (VGRAD(I)/VE(I) + YP(1)/YT(1))
     +      + .0306 * (H1 - 3.)**(-.6169)/YT(1)
      RETURN
      END

c=====================================================================

      SUBROUTINE RUNGE2(I0,I1,DX,YY,N)
c
c     2ND-ORDERRUNGE-KUTTA METHOD FOR SYSTEM OF N FIRST
c     ORDER EQUATIONS
c

      DIMENSION YS(200),YY(200)
      COMMON /RNK/ YT(200),YP(200)

      INTVLS = I1-I0
      IF (INTVLS .LT. 1)  GOTO 200
      DO 130 I=1,INTVLS
      DO 100 J=1,N
100   YT(J) = YY(J)
      CALL DERIVS(I0 + I - 1)
      DO 110 J=1,N
        YT(J) = YY(J) + DX * YP(J)
110   YS(J) = YY(J) + .5 * DX * YP(J)
      CALL DERIVS(I0 + 1)
      DO 120 J=1,N
120   YY(J) = YS(J) + .5 * DX * YP(J)
```

```
130     CONTINUE
200     RETURN
        END
```

```
c234567890123456789012345678901234567890123456789012345678901234567890123456789012
c
c       SMHESS.FOR
c       This program uses the Smith-Hess panel method to calculate
c       the flowfield about an arbitrary 2D body in an ideal flow.
c
c                Written by Dr. A Arena 10 November, 1993
c
c**********************************************************************

        program smhess

        real ep(200,2), ept(200,2), pt1(200,2), pt2(200,2)
        real co(200,2), a(200,200), b(200,200), g(200)
        real th(200),pi

        pi=4.*atan(1.)

        open(8,file='cps.dat')

        write(*,*)'Enter number of panels'
        read(*,*)m
        write(*,*)'enter angle of attack in deg.'
        read(*,*)alphd

        alpha = pi*alphd/180.
        n = m + 2

c       Read in the panel end points, using subroutine body, or an
c       external geometry file created by the user

        write(*,*)'create airfoil or read file (0/1)'
        read(*,*)irpl
          if(irpl.eq.1)then
        open(4,file='afoil.dat',status='old')
        do i=1,m+1
         read(4,*)ept(i,1),ept(i,2)
        end do
        close(unit=4)
      else
         call body(m,ept)
          endif

c       Convert panelling to clockwise

        do i=1,m+1
          ep(i,1)=ept(m+1-i+1,1)
          ep(i,2)=ept(m+1-i+1,2)
        end do

c       Establish coordinates of panel end points

        do i=1,m
          pt1(i,1)=ep(i,1)
```

```
      pt2(i,1)=ep(i+1,1)
      pt1(i,2)=ep(i,2)
      pt2(i,2)=ep(i+1,2)
      end do

c     Find panel angles th(j)

      do i=1,m
      dz=pt2(i,2)-pt1(i,2)
      dx=pt2(i,1)-pt1(i,1)
      th(i)=atan2(dz,dx)
      end do

c     Establish collocation points

      do i=1,m
      co(i,1)=(pt2(i,1)-pt1(i,1))/2+pt1(i,1)
      co(i,2)=(pt2(i,2)-pt1(i,2))/2+pt1(i,2)
      end do

c     Establish influence coefficients

      do i=1,m
      uv=0.
      wv=0.
      do j=1,m

c     Convert collocation point to local panel coordinates
      xt=co(i,1)-pt1(j,1)
      zt=co(i,2)-pt1(j,2)
      x2t=pt2(j,1)-pt1(j,1)
      z2t=pt2(j,2)-pt1(j,2)

      x=xt*cos(th(j))+zt*sin(th(j))
      z=-xt*sin(th(j))+zt*cos(th(j))
      x2=x2t*cos(th(j))+z2t*sin(th(j))
      z2=0.

c     find r1, r2, th1, th2
      r1=sqrt(x**2+z**2)
      r2=sqrt((x-x2)**2+z**2)

      th1=atan2(z,x)
      th2=atan2(z,x-x2)

c     Compute velocity in local panel reference frame

      if(i.eq.j) then
      ul=0.
      wl=0.5
      ulv= 0.5
      wlv= 0.
      else
      ul=1./(2.*pi)*log(r1/r2)
```

```
        wl=1./(2.*pi)*(th2-th1)
        ulv = 1./(2.*pi)*(th2-th1)
        wlv = 1./(2.*pi)*log(r2/r1)
      end if

c     Return velocity to global reference frame
      u=ul*cos(-th(j))+wl*sin(-th(j))
      w=-ul*sin(-th(j))+wl*cos(-th(j))
      uv = uv + ulv*cos(-th(j)) + wlv*sin(-th(j))
      wv = wv - ulv*sin(-th(j)) + wlv*cos(-th(j))


c     a(i,j) is the influence coefficient defined by the
c     tangency condition.  b(i,j) is the induced local
c     tangential velocity to be used in Cp calculation

      a(i,j)=-u*sin(th(i))+w*cos(th(i))
      b(i,j)=u*cos(th(i))+w*sin(th(i))

       end do

      a(i,m+1) = -uv*sin(th(i)) + wv*cos(th(i))
      b(i,m+1) = uv*cos(th(i)) + wv*sin(th(i))

c     RHS

      a(i,n)=cos(alpha)*sin(th(i))-sin(alpha)*cos(th(i))

      end do

c     KUTTA condition

      do j=1,m+1
        a(m+1,j) = b(1,j) + b(m,j)
        a(m+1,m+2) = - ( cos(alpha-th(1)) + cos(alpha-th(m)) )
      end do

c     Solve for solution vector

      call matrx(a,n,g)

c     Convert source strengths into tangential velocities
c     along the airfoil surface and Cp's on each panel


      do i=1,m
        vel=0.
        do j=1,m+1
          vel=vel+b(i,j)*g(j)
        end do
        cp=1.-(vel+cos(alpha-th(i)))**2
        write(8,*)co(i,1),',',cp
      end do
```

```
      close(unit=8)
      stop
      end

c=====================================================================

      subroutine matrx(a,n,g)

c           matrx is a matrix reducer of the Gaussian type
c           a(i,j) is the matrix, g(i) is the solution vector

      real a(200,200),temp(200,200),g(200)


c           initialize the g vector to all zeros

      do i=1,n-1
       g(i)=0.
      end do

c           convert coefficient matrix
c           to upper triangular form

 5    do i=1,n-1
       if(abs(a(i,i)).lt.0.0000001)goto 9

      p=a(i,i)
      do j=i,n
       a(i,j)=a(i,j)/p
      end do

      do k=i+1,n-1
       p2=a(k,i)
       do l=i,n
        a(k,l)=a(k,l)-p2*a(i,l)
       end do
      end do
      end do

c           back substitute triangularized matrix to get
c           values of solution vector

      do i=n-1,1,-1
       g(i)=a(i,n)
       do j=1,n-1
        a(i,i)=0.
       g(i)=g(i)-a(i,j)*g(j)
       end do
      end do

      return

c           order matrix so that diagonal coefficients are
c           not=0 and stop if matrix is singular
```

```
 9      if(i.ne.n-1)then
         do j=1,n
          temp(i,j)=a(i,j)
          a(i,j)=a(i+1,j)
          a(i+1,j)=temp(i,j)
         end do
         goto 5
        else
         goto 10
        end if

 10     write(*,*)' NO SOLUTION '

        stop
        end

c=======================================================================

        subroutine body(m,ept)

c               this subroutine calculates the nodal coordinates
c               of the body surface panels for a NACA symmetric
c               airfoil. Data is nondimensionalized by chord
c       *** NOTE: PANEL 1 @ TE. TOP SFC., NUMBERING SCHEME
c             COUNTER-CLOCKWISE                                  ***

        real pi,pthick,eps,theta,xc,thick,z,ept(200,2)

        pi=4.*atan(1.)

c       pthick is percent thickness/chord of the airfoil.
c       eg. pthick=12 for a NACA 0012 airfoil

        pthick = 12.
        eps = pthick/10.

        do i=1,1+m
         theta=2.*pi*float(i-1)/float(m)
         xc =  ( 1. + cos(theta) )/2.
        thick = eps*(.2969*sqrt(xc) - .126*xc - .3537*xc**2
     &      + .2843*xc**3 - .1015*xc**4)
        z = thick*sign(1.,sin(theta))/2.

        ept(i,1)=xc
        ept(i,2)=z

        end do

        return
        end
```

• CODE VALIDATION

Experimental data of NACA4412, NACA65,2-421 and NACA66,2-420 airfoils have been used to validate the three code developed for the current study. The calculated results by these three codes were compared with those calculated by Cebeci [19] and the results observed in experimental data [19].

Based on the results following, it was concluded that these codes were validated. Though digitizing experimental data was done in a rough manner, the calculated results still have a good agreement with Cebeci's data as well as experimental data.

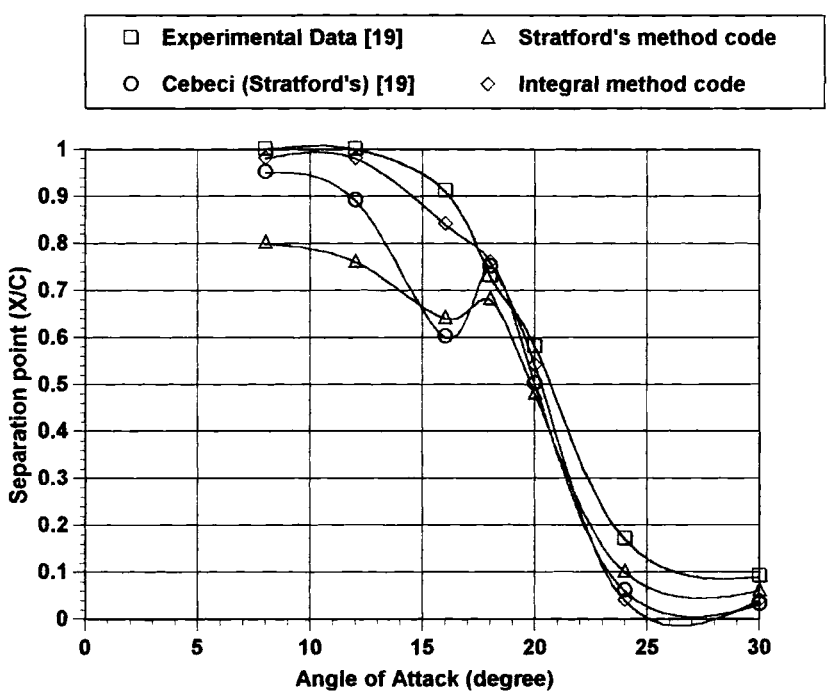

Figure A.1 Code validation with NACA4412, Re=3,000,000

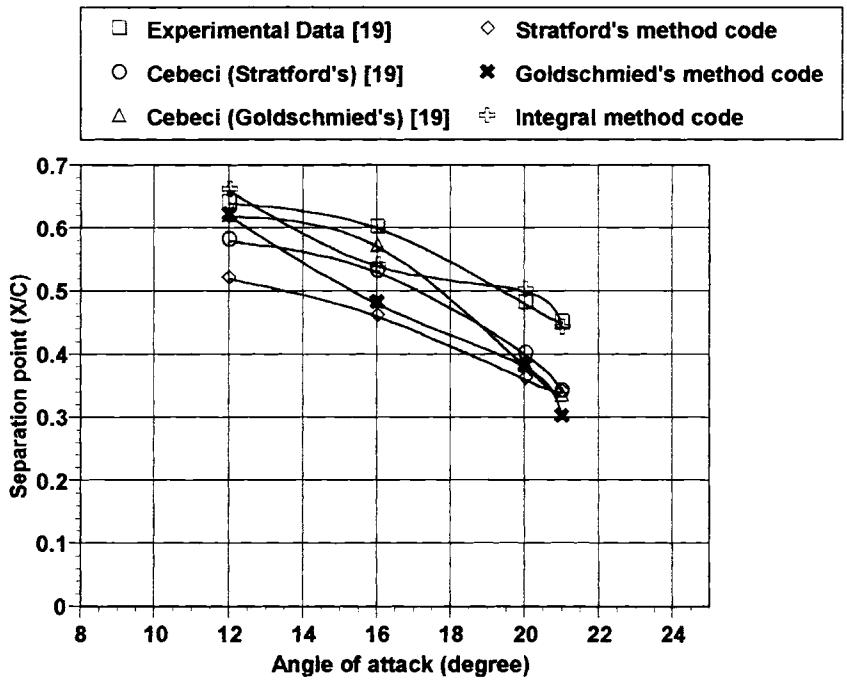

Figure A.2 Code validation with NACA65,2-421 , Re=6,000,000

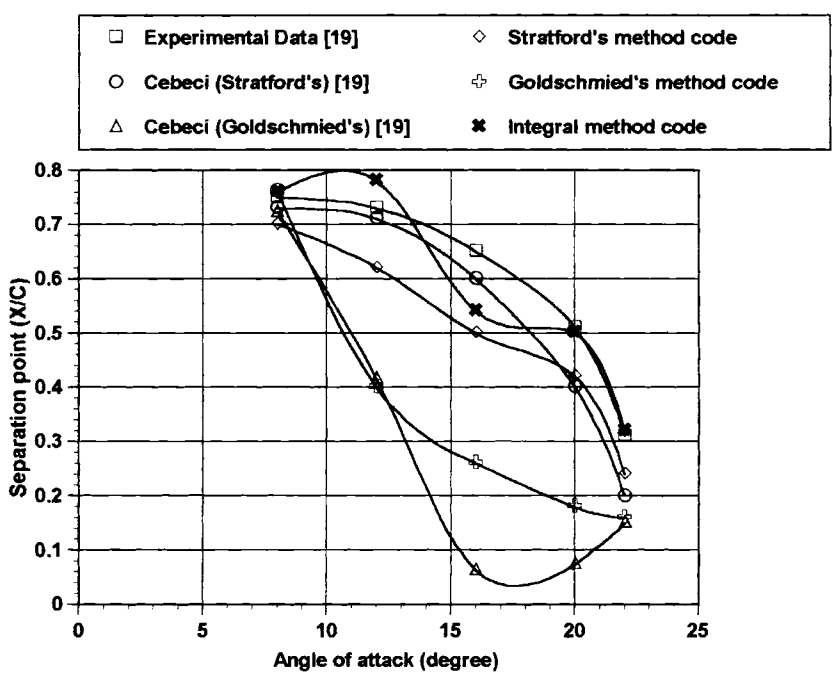

Figure A.3 Code validation with NACA66,2-420, Re=6,500,000

VITA

Takamasa Kai

Candidate for the Degree of

Master of Science

Thesis: A SURVEY OF SEPARATION PREDICTION METHODS APPLIED TO POTENTIAL FLOW SOLUTIONS FOR AN AIRFOIL

Major Field: Mechanical Engineering

Biographical:

Personal Data: Born in Tokyo, JAPAN, On July 17, 1966, the son of Shinei and Haruko Kai.

Education: Graduated from Keio High School, Yokohama, JAPAN in March 1985; received Bachelor of Engineering degree in Mechanical Engineering from Keio University, Tokyo, JAPAN in March 1989. Completed the Requirements for the Master of Science degree with a major in Mechanical Engineering at Oklahoma State University, Stillwater, Oklahoma in July 1995.

Experience: Employed by Oklahoma State University, Department of Mechanical and Aerospace Engineering as a graduate research assistant and a graduate teaching assistant; Oklahoma State University, 1993 to present.

Professional memberships: Sigma Gamma Tau Aerospace Honor Society.